ISSN: 1863-5598

ZKZ 64717
01-25

Bodo´s Power Systems®

Electronics in Motion and Conversion

January 2025

PULSED INDUCTANCE MEASUREMENT

POWER CHOKE TESTER DPG10/20 SERIES

Inductance measurement from 0.1 A to 10 kA

KEY FEATURES

Measurement of the

- **Incremental inductance** $L_{inc}(i)$ and $L_{inc}(\int Udt)$
- **Secant inductance** $L_{sec}(i)$ and $L_{sec}(\int Udt)$
- **Flux linkage** $\psi(i)$
- **Magnetic co-energy** $W_{co}(i)$
- **Flux density** $B(i)$
- **DC resistance**

Also suitable for 3-phase inductors

WIDE RANGE OF MODELS

7 models available with maximum test current from 100A to 10000A and maximum pulse energy from 1350J to 15000J

KEY BENEFITS

- Very **easy and fast** measurement
- **Lightweight, small and affordable price-point** despite of the high measuring current up to 10000A
- **High sample rate and very wide pulse width range** => suitable for all core materials

APPLICATIONS

Suitable for all inductive components from **small SMD inductors** to **very large power reactors in the MVA range**

- **Development, research** and **quality inspection**
- **Routine tests** of small batch series and mass production

Technological leader in pulsed inductance measurement for 18 years

www.ed-k.de

Content

Supporters & Friends

A Media
Katzbek 17a
24235 Laboe, Germany
Phone: +49 4343 42 17 90
Fax: +49 4343 42 17 89
info@bodospower.com
www.bodospower.com

Founder
Bodo Arlt, Dipl.-Ing.
bodo@bodospower.com

Editor in Chief
Alfred Vollmer, Dipl.-Ing.
alfred@bodospower.com

Correspondent Editor Bavaria
Roland R. Ackermann, Dipl.-Ing.
roland@bodospower.com

Editor China
Min Xu – xumin@i2imedia.net

US Support
Rusty Dodge
rusty@eetech.com

Creative Direction & Production
Bianka Gehlert
b.gehlert@t-online.de

Publisher
Holger Moscheik
holger@bodospower.com

Free Subscription to qualified readers
Bodo´s Power Systems is available for the following subscription charges:
Annual charge (12 issues) is
150 € world wide · Single issue is 18 €
subscription@bodospower.com

Printing by:
Dierichs Druck+Media
GmbH & Co. KG,
34121 Kassel, Germany

What an Event!

In a response to our post on LinkedIn where we thanked all the contributors to Bodo's Wide Bandgap Event one person commented "Great format, and I loved the 15-minute sessions – I felt I'd been hit with a fire-hose of WBG knowledge." I personally wouldn't have been able to express it in a more precise way. So, I think that the entire team of Bodo's Power Systems can surely say "Mission Accomplished".

When I moderated the SiC session on day #2 at our WBG event, I quoted Guy Moxey (Wolfspeed), who said the following at the panel discussion on day #1: "Use SiC as a weapon with an incredible value for money," because I think he is right. He talked about the price decline of a specific SiC component which cost $85 ten years ago, which we can now buy in volumes for $3.50. However, I'd like to extend this to GaN as well because considering the entire system and lifetime cost of both, SiC and GaN designs, these technologies are able to provide "an incredible value for money".

Aly Mashaly (ROHM) told us that "in 2030 all the servers in the world will consume six times the entire power consumption of Germany". Considering that Germany has climbed to the 3rd place in the global GDP rankings of national economies (after the US and China) in 2024 this is an almost incredible amount of power consumption for a single application class. This and other data and details discussed clearly demonstrates how important it is to develop real energy-saving systems.

During Bodo's WBG Event we saw so many excellent approaches making the best out of the huge energy demand, and we will continue to bring you many inspiring power solutions – hopefully highly efficient solutions – in the twelve magazines we have planned for 2025. Bodo and I are both electrical engineers, but we are unable to write so many in-depth power stories per year nor can we present 40 technical WBG papers in a single day, nor can we explain products in the tabletop exhibition. Therefore, we really appreciate your help and support for writing stories, for presenting at our event and for inspiring us at trade shows and conferences. This is why we say thank you very much for all of your support. Let's continue to co-operate in a fruitful way in 2025! Keeping this in mind the entire team of Bodo's Power Systems wishes you a healthy, inspiring, prosperous and peaceful 2025!

Bodo's magazine is delivered by postal service to all places in the world. It is the only magazine that spreads technical information on power electronics globally. We have EETech as a partner serving our clients in North America. If you speak the language, or just want to have a look, don't miss our Chinese version at bodospowerchina.com. An archive, of every issue of the magazine, is available for free at our website bodospower.com.

My green tip of the month: Use the WBG "weapon" (or is it better we call it a "seed"?) to create highly-efficient power systems. As every percentage point increase in power efficiency counts!

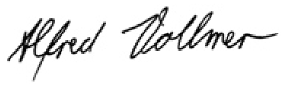

Events

NEPCON Japan 2025
Tokyo, Japan January 22 -24
www.nepconjapan.jp

DesignCon 2025
Santa Clara, CA, USA January 28 – 30
www.designcon.com

PLECS Conference 2025
Zurich, Switzerland March 4 – 5
www.plexim.com/events

embedded world 2025
Nuremberg, Germany March 11 -13
www.embedded-world.de

APEC 2024
Atlanta, GA, USA March 16 – 20
www.apec-conf.org

AMPER 2025
Brno, Czech Republic March 18 – 20
www.amper.cz

SEMICON China 2025
Shanghai, China March 26 – 28
www.semiconchina.org

Battery Tech Expo 2025
Silverstone, UK March 26 – 27
https://batterytechexpo.co.uk

EPE 2025
Paris, France March 31 – April 4
https://epe2025.com

Acquisition of SiC JFET Business

onsemi announced that it has entered into an agreement to acquire the Silicon Carbide Junction Field-Effect Transistor (SiC JFET) technology business, including the United Silicon Carbide subsidiary, from Qorvo. The acquisition will complement onsemi's extensive EliteSiC power portfolio and enable the company to address the need for high energy efficiency and power density in the AC-DC stage in power supply units for AI data centers. Additionally, the move will accelerate onsemi's readiness for emerging markets such as EV battery disconnects and solid-state circuit breakers (SSCBs). "As AI workloads become more complex and energy-intensive, the importance of reliable SiC JFETs that deliver high energy efficiency and are able to handle high voltages will continue to increase," said Simon Keeton, group president and general manager of the Power Solutions Group, onsemi. "With the addition of Qorvo's industry leading SiC JFET technology, our intelligent power portfolio offers our customers yet another solution to optimize energy consumption and increase power density."

www.onsemi.com

Cooperation for Development of Sensor ICs with Functional Safety

Novosense Microelectronics and Continental Automotive Technologies have signed a memorandum to enhance strategic cooperation in the development of sensor ICs with functional safety, as well as for the global integration of Novosense's products within Continental's worldwide platforms. Products being co-developed include those for safety functions and system reliability – from airbag triggers to battery pack monitors. Novosense is a member of the AEC and an active developer for the global automotive industry. It has implemented an extensive R&D program for the sector that leverages a system-level understanding of automotive electronics, as well as a reliable product delivery supply chain.

www.novosns.com

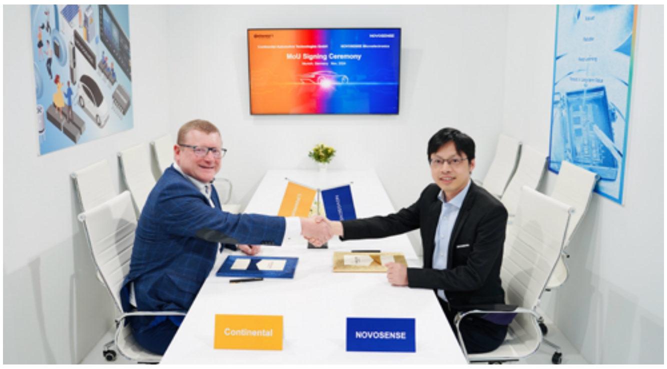

SiC Partnership between Automotive OEM and Semiconductor IDM

STMicroelectronics and Renault Group's Ampere have entered a multi-year agreement, effective from 2026, for the supply of Silicon Carbide (SiC) power modules. The multi-year agreement is aligned with Ampere's strategy of working upstream with its partners. The two companies have worked together on the optimization of a new power module, the key element in the powerbox. The powerbox combines three SiC-based power modules, an excitation module, which provides the necessary electrical excitation to the motor or generator for controlling the magnetic field within the motor, and a cooling baseplate designed to dissipate heat from the back side of the power module, simplifying the thermal management and cooling process. It is designed for both 400 V and 800 V battery systems, with the latter allowing rapid charging from 10% to 80% in under 15 minutes.

www.st.com

Semiconductor Product Distribution Center opened in Germany

Texas Instruments has opened its product distribution center in Dreieich, Germany, close to Frankfurt, Germany. This distribution center includes 9,000 square meters of space and specific automation features. It has the capacity to quickly ship up to 7,500 orders per day. Located near Frankfurt Airport, the distribution center enables faster product delivery in Europe. The pick, pack and ship process is fully automated and orders are ready to ship within 15 minutes or less. Customers in central Germany can expect same-day product delivery, while next-day delivery is available to customers in most European countries. TI has been operating in Europe since 1956.

www.ti.com

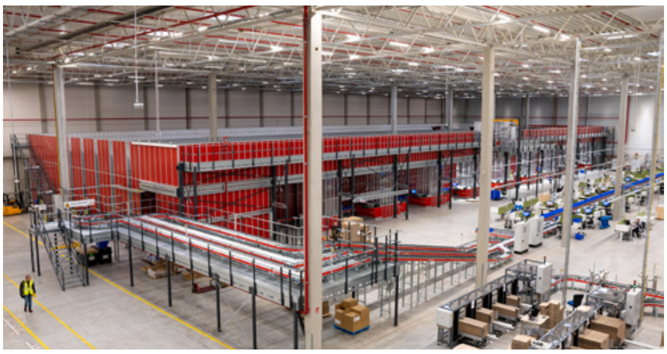

Collaboration to Advance Plug & Charge

Vector and Hubject now collaborate to further advance the Plug & Charge (PnC) technology. The aim is to simplify the electric vehicle (EV) charging process. With more than 2.6 million PnC-ready vehicles already on the market and more EVs on the horizon, the partnership helps to accelerate the adoption and implementation of PnC technology. Through this collaboration, automotive OEMs and charging station manufacturers can now obtain the Hubject QA (Pre-Production) and Production Certificates via the Vector Security Manager with the latest release of the development and test tool CANoe Version 18 SP3. The Vector Security Manager is the link between the Vector tools and the OEM-specific security implementations. With it, security functions can be used uniformly in the tools. Hubject QA and Production Certificates are essential for testing EVs and Electric Vehicle Supply Equipment (EVSE) using the CANoe Test Package EV or CANoe Test Package EVSE from Vector. This integration ensures that both the vehicles and the charging stations meet the ISO 15118 standard of interoperability, conformity and market readiness. PnC offers a seamless user experience. It eliminates the need for physical cards or mobile apps to authenticate and initiate charging.

www.vector.com

TSMC Excellent Performance Award

Asahi Kasei received a 2024 TSMC Excellent Performance Award for its Pimel™ photosensitive Polyimide material, in recognition of its "Excellent Technology Collaboration and Production Support in Advanced Packaging" at the 2024 Supply Chain Management Forum held by Taiwan Semiconductor Manufacturing.

TSMC presents the Excellent Performance Award to suppliers that have made remarkable contributions to its technology leadership and manufacturing with advanced semiconductor processes over the past year. At the award ceremony, TSMC Chairman & CEO Dr. C.C. Wei thanked suppliers for delivering timely and high-quality professional services to drive continuous improvement of the supply chain and related industries. Pimel™ has been used for worldwide semiconductor applications such as buffer coatings, passivation layers for bumping, and dielectric layers for re-distribution bumping. As semiconductor technology continues to advance, the demand for materials like Pimel™ has grown, with these applications becoming increasingly vital in supporting the evolution of more complex and compact semiconductor devices.

www.asahi-kasei.com

GaN Design and Development Center in Ottawa, Canada

The French company Wise-integration, which is active in digital control of gallium nitride (GaN) and GaN ICs for power conversion, has opened its North American Design & Development Center in Ottawa, Ontario, Canada. Led by Christian Cojocaru and staffed by experts in analog and digital technology design, the center will drive the development of the company's design portfolio for the next generations of WiseGan®. By maximizing the high-frequency capabilities of GaN without added power losses, the next generations of the two product lines are said to "enable significant reductions in system size and cost, while boosting overall conversion efficiency". Since its launch in 2020, the fabless company has established more than 20 patent families for its two core product lines. WiseGan includes GaN power integrated circuits designed for high-frequency operation in the MHz range, integrating features that streamline implementation with digital control. WiseWare is a 32-bit, MCU-based AC/DC digital controller optimized for GaN-based power-supply architectures. The company recently announced the launch of a subsidiary in Hong Kong.

www.wise-integration.com

A very short Look back at electronica 2024

From November 12 to 15,2024 a total of 3,480 exhibitors presented their innovations across the entire spectrum of electronics to about 80,000 visitors at the electronica trade fair in Munich, Germany. In addition to sustainability, key topics such as artificial intelligence, the future of mobility, and the development of young talent

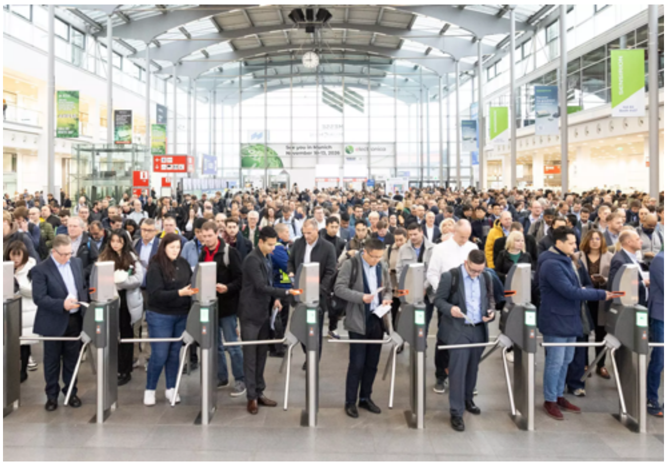

sparked discussions at the exhibition stands and at the supporting program. The equally successful SEMICON Europa took place concurrently in two of the 18 halls. The organizer, Messe München, is "delighted that the trade fair was once again held at the same high level as before the pandemic and that the atmosphere was very positive despite the challenging times". In order to attend electronica show, which had its debut exactly 60 years before, 3,480 exhibitors traveled from 59 countries and regions, with 76 percent of them from abroad. There were around 80,000 visitors from around 100 countries and regions. The share of international visitors totaled 54 percent. After Germany, the top 10 visitor countries were: Italy, China, France, Austria, United Kingdom, Switzerland, USA, Spain, Netherlands and Poland.

Some trivia: Roland R. Ackermann, the Correspondent Editor Bavaria of Bodo's Power Systems, had already visited the very first electronica show 60 years ago while he was delighted to greet so many friends and business friends at this year's electronica show as well. The next electronica will take place from November 10 to 13, 2026.

www.electronica.de

"A much better Way to conduct Heat away from the Die" – especially in GaN Applications

QPT has just filed a patent for a way to attach dies to the heat spreaders or substrates which are typically Aluminium Nitride (AlN), which it calls *qAttach*™. This is said to provide "a much better way to conduct heat away from the die and also increases reliability" as the assembly process places less stress on the substrates, which is one of the biggest challenges the high-power semiconductor packaging industry faces. QPT developed this *qAttach* process for use with the Gallium Nitride (GaN) transistors that it uses in its electric motor control designs to enable them to handle the huge amounts of waste heat that results from using them for high power, high voltage applications and at high frequency. GaN transistors are now being made that are rated for high voltages but the die size is relatively small for high voltage transistors, which means there is less surface area to remove heat from. As a result, they are often down rated to enable them to function without overheating. *qAttach* solves this problem as now significantly more heat can be efficiently removed from the die so that it will not overheat. This opens up GaN to now be efficiently used for next generation, high power, high voltage applications in automotive, industrial motors and to finally deliver on the promise of low cost, high voltage GaN transistors.

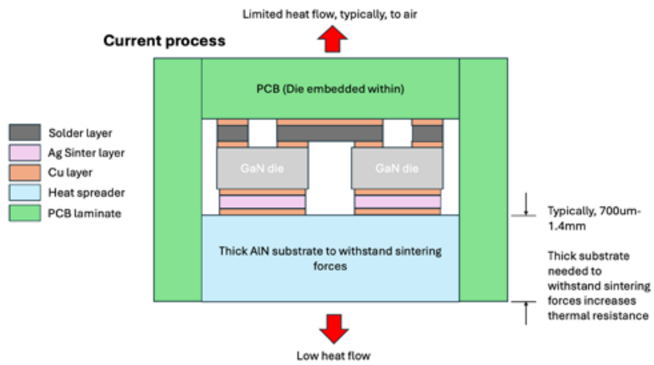

www.q-p-t.com

Semiconductor Company cooperates with Automotive Tier-1 Supplier

ROHM Semiconductor and Valeo announced they are collaborating to propose and optimize the next generation of power modules for electric motor inverters using their combined expertise in power electronics management. As a first step, ROHM will provide its 2-in-1 Silicon Carbide (SiC) molded module TRCDRIVETM pack to Valeo for future powertrain solutions. Valeo focuses on efficient, electrified mobility across various vehicle types and markets from the smallest one (ebikes), through the mainstream (passenger cars) to the largest one (eTrucks).

ROHM and Valeo have been collaborating since 2022, initially focusing on technical exchanges aimed at improving the performance and efficiency of the motor inverter. By refining power electronics, both companies aim to offer optimized cost/performance by delivering higher energy efficiency, reducing heat generation thanks to an optimized cooling and mechatronic integration, and increasing overall reliability with a SiC packaging. Valeo will start supplying a first series project in early 2026.

www.rohm.com

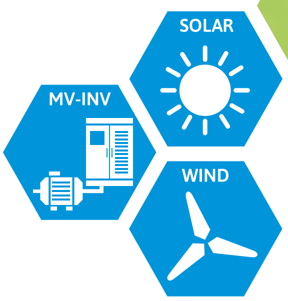

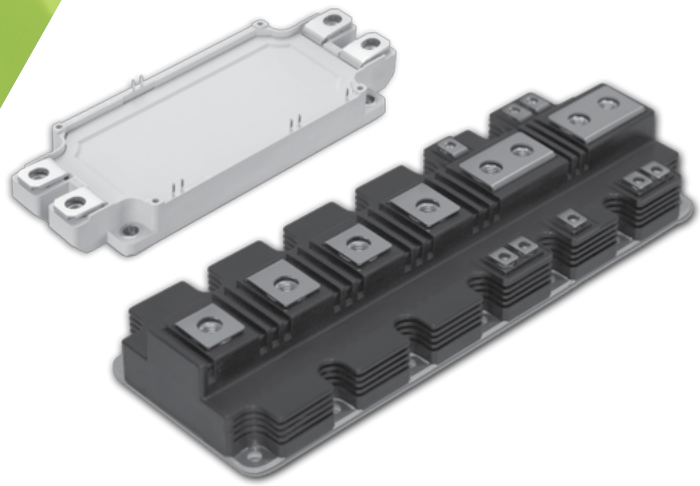

Reverse Conducting IGBT (RC IGBT)

2400A/1200V & 2400A/1700V in PP3+
1000A/1200V & 800A/1700V in DualXT

FEATURES

- RC technology is combining IGBT and FWD in the same chip
- Improved solder material for higher reliability
- Higher lifetime at same ΔT*j*
- Increased output power
- Higher power cycling capability
- Lower conducting and switching losses

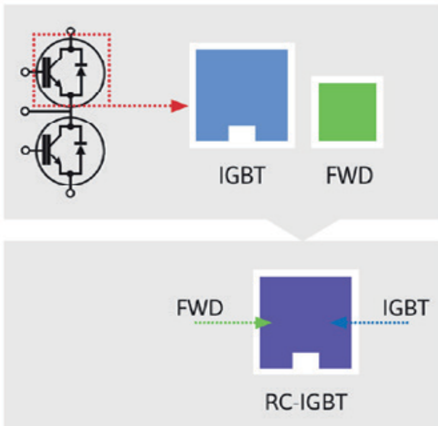

Donation to Charity instead of Christmas Gifts

Vincotech has again opted to embrace the seasonal spirit of charity. In lieu of sending gifts to customers, the company is presenting 12,000 Euros to its partner in philanthropy, Plan International Germany. Donated on behalf of its workforce and customers, these funds will support a development project in Ecuador. Youngsters, and girls especially, in ten communities in the Cotopaxi and Santa Elena regions stand to benefit from this initiative. It aims to impart business, digital, and soft skills that will help get them off to a better start in working life. The project also provides health services to mothers and children. This is Vincotech's second contribution to the project. The company had staged a virtual reality challenge at the PCIM Europe trade fair in May 2024 to raise funds for Plan International Germany. Fairgoers rose to the occasion. Vincotech and its partners rewarded their efforts by pledging €15,000 to upskill young Ecuadorians and furnish health services.

www.vincotech.com

Chief Operating Officer started in Office

Markus Fischer, the former Executive Vice President Operations, has been appointed to the Rohde & Schwarz Executive Board. As Chief Operating Officer (COO), he will collaborate with Christian Leicher (CEO) and Andreas Pauly (CTO) to continue to keep the company on course for growth in these challenging times. As Chief Operating Officer, Markus Fischer will be responsible for most of the operative business of Rohde & Schwarz. Andreas Pauly, who joined the Executive Board as Chief Technology Officer in October 2023, will retain his primary responsibility for innovation, research and development. Managing Partner Christian Leicher will continue to head the Executive Board as President and CEO. Markus Fischer (44) joined the technology group in 2011 as Head of Corporate Material Sourcing at Munich headquarters. After another management role at Rohde & Schwarz Messgerätebau GmbH in Memmingen, he assumed overall responsibility for the group's supply chain in 2017. In July 2020, he was appointed Executive Vice President Operations, becoming a member of Corporate Management. In that role, Fischer was responsible for all Rohde & Schwarz production activities as well as the supply chain and procurement. The technology group's five production plants have a high degree of vertical integration. As Executive Vice President Operations, Fischer focused above all on improving such key aspects as efficiency, flexibility and scalability. Consequently, his division not only ensured delivery capability in times of uncertain supply chains, but also contributed substantially to the stability of Rohde & Schwarz.

www.rohde-schwarz.com

Acquisition in Current Sensor Business

Isabellenhütte Heusler has acquired Rathgeber. Both companies have a long-standing business relationship: As an external manufacturing service provider, Rathgeber was entrusted by Isabellenhütte with the punching of resistance bands, from which the ISA-WELD resistor series for current measurement is manufactured. Isabellenhütte expects to gain a strategic advantage from the acquisition. Rathgeber specializes in the production of temperature regulators for various markets. Isabellenhütte can thus supplement its product portfolio in measurement technology, expand its manufacturing expertise and strengthen its competitiveness.

www.isabellenhuette.com

Three Companies partner for Solar Inverter Designs

Mouser Electronics has partnered with onsemi and Würth Elektronik to address the growing solar inverter market. onsemi's Silicon Carbide (SiC) solutions address the needs for the highest levels of efficiency, reliability, and safety while their boost and inverter power integrated modules (PIMs) anchor the grid-interface electronics. Würth Elektronik's gate drivers, sensing control, and peripheral power products complete the system. E. g. the onsemi NXH40B120MNQ1 is an EliteSiC PIM containing a dual full SiC boost stage. The Würth Elektronik WE-AGDT high-power auxiliary gate drive transformers feature unipolar and bipolar outputs, making them suitable for powering state-of-the-art SiC MOSFET gate drivers up to 6W of power as well as IGBT and power MOSFETs.

www.mouser.com

More Power by RC-IGBT Technology

Fuji Electric introduces a new rating in a well-known package to increase the output power of IGBT modules by applying "RC-IBGT" (RC for Reverse Conducting) technology for high-power applications

By Oleksii Khruniak, Field Application Engineer, Fuji Electric Europe

Introduction

In previous years, Fuji Electric has introduced RC-IGBT in well-known packages with the objective of enhancing the output power of existing systems using IGBT modules. This well-known "RC-IBGT" (RC stands for reverse conducting) technology for high-power applications has already found its way into the market several years ago. The addition of RC-IGBT technology to already existing packages of PrimePACK™3+, DualXT, PC2/3 and Small PIM2 brings the system design flexibility so needed to follow shifting market trends (Figure 1).

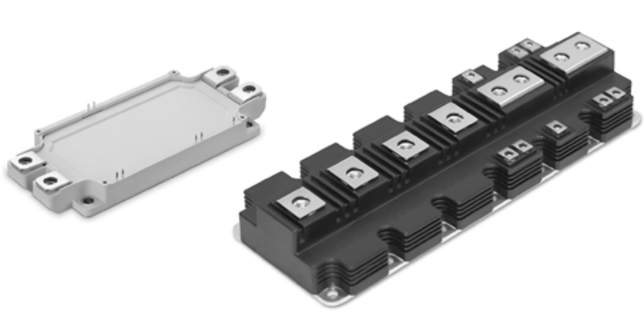

Figure 1: DualXT and PrimePACK™3+

The market demand for power semiconductors has been increasing for several years, driven by the need for miniaturisation of power conversion systems, reduction of costs and performance improvement. Such an enhancement in performance is attained by expanding the output power within a fixed package size, which concurrently leads to rising operation temperatures within the system. Higher operating temperatures lead to an increased risk of a shorter product lifetime, due to a reduction in the number of power cycles that can be performed at higher temperatures.

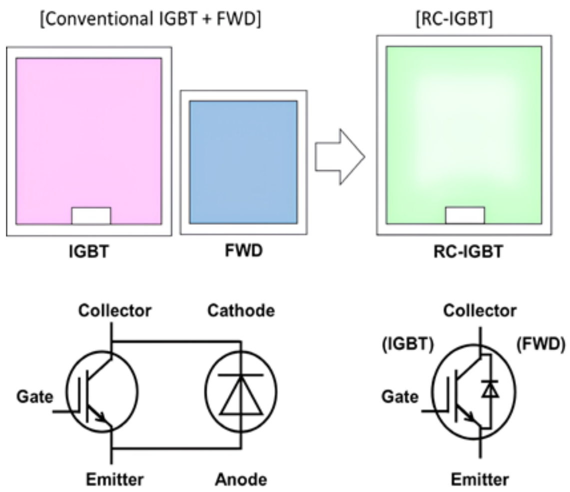

Figure 2: Schematic diagrams of the X series RC-IGBT and equivalent

Fuji Electric accepted the challenge of developing chips and packages capable of withstanding these higher performance levels without compromising the module lifetime, and presented the 7th generation of IGBT module technology, the "X-series", some years ago. The combination of high-power density and high reliability is achieved by reducing power dissipation.

Moreover, Fuji Electric developed the RC-IGBT technology, which integrates IGBT and FWD in a single chip. This allows for a reduction in the number of chips and the chip area required, while maintaining the same level of rated current. Furthermore, it is possible to achieve higher currents.

This results in an increase of the rated current in the same package size and a reduction in power dissipation by combining the X series technology with the RC-IGBT technology. The reliability of the portfolio exceeds that of conventional IGBT modules.

RC-IGBT technology

The RC-IGBT technology involves the integration of IGBT and FWD patterns on a single chip (Figure 2). The proportion of active area to the total chip area is increased as a consequence of the reduction in the chip's edge termination, which generates additional space within the module housing for larger chips, thereby enabling an enhanced output current. Furthermore, the extended chip area has the effect of reducing the thermal resistance between the junction and the case, Rth(j-c), to a considerable extent. The larger chip area functions as a thermal buffer zone, facilitating the transfer of generated heat from the IGBT region to the FWD region and vice versa. Consequently, the I^2t capability of the RC-IGBT is almost 4 times greater than that of the predecessor V series generation.

In the figure 3 a trade-off in junction temperature swing from Fuji Electric PrimePACK™3+ 2400A/1200V RC-IGBT X-series module and PrimePACK™3+ 1800A IGBT X-series module is shown.

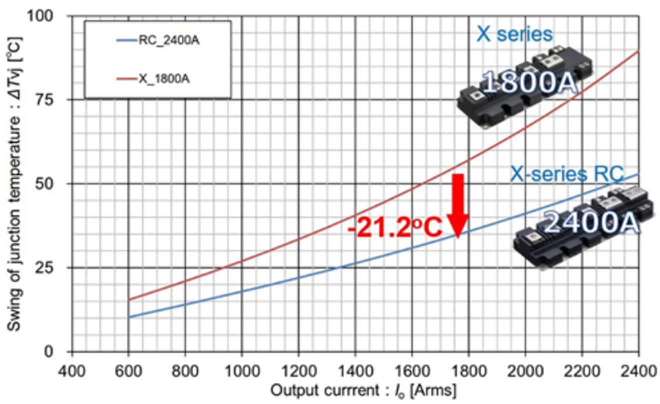

Figure 3: Calculation conditions: Io=Vari., fc=3 kHz, fo=1 Hz, Vcc=600 V, pf=0.9, m=0.01, nominal RG, Rth(s-a)=6 K/kW, Rth(c-s)=1.4 K/kW(with 3 W thermal grease), Ta=50 °C

Erik Rehmann, GVA expert for Quality Management

gva-power.de

In a large-scale grid-connected photovoltaic system, IGBT modules are typically connected in parallel to increase the output current. This topology typically necessitates a considerable amount of system space and a meticulously devised electrical configuration with minimal current imbalances. Photovoltaic (PV) systems operate normally at relatively constant power. In instances where two 1400A V-series PrimePACK™ units were previously employed or one 1800A X-series IGBT, they can now be substituted with a single 2400A RC-IGBT module, thereby reducing the footprint by half or expanding power output.

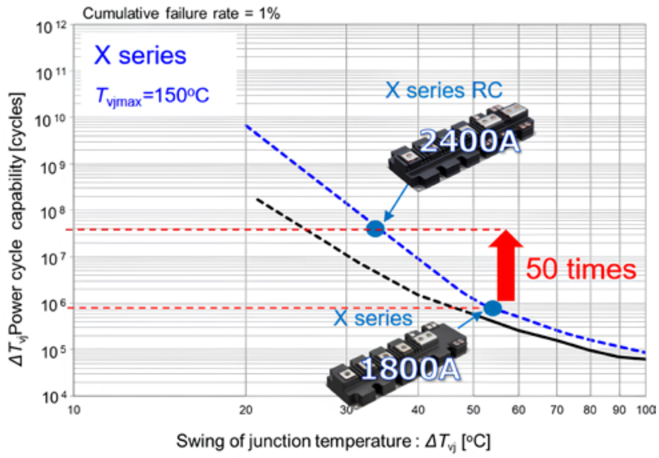

Figure 4: 1200V PrimePACK™3+ ΔTvj Power cycle lifetime comparison Io=1800Arms

High-power drive system have a low output frequency during the initial motor start-up. This is the most critical phase, given that the load is sustained on a single chip for a relatively long time. The resulting high temperature swings induce thermal stress on the die attach and bonding wire connections, which ultimately results in a reduction in the power cycling lifetime.

The application of RC-IGBT technology and its larger relative chip area results in a significant reduction in temperature swings, thereby extending the device's operational lifetime. The expected life time of the 2400A RC-IGBT module will be much higher in this case (Figure 4).

Figure 5 shows the reduction of the temperature swing of a X Series 2400A/1700V PrimePACK™3+ RC-IGBT compared to a X Series 1800A/1700V.

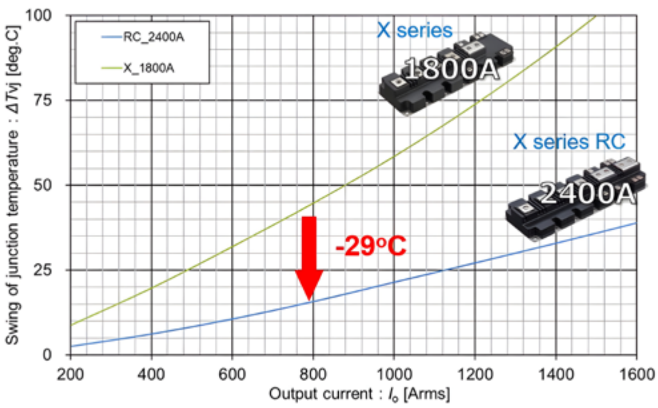

Figure 5: Calculation conditions: Io=Vari., fc=3kHz, fo=5Hz, Vcc=1200V, pf=-0.9, m=1, Standard RG, Rth(s-a)=4.7°C/kW, Rth(c-s)=1.4°C/kW (with 3W thermal grease), Ta=35°C

First, on the generator side, an inverter converts the rotational movement of the wind turbine, which provides alternating current (AC) electric power, into direct current (DC) electric power. The turbine rotates slowly, resulting in significant stress on the IGBT and FWD due to the high load. RC-IGBT chips are capable of preventing significant temperature fluctuations.

Second, on the grid side, the electrical power is converted back to alternating current (AC) and fed into the grid network.

The two sides have distinct roles to fulfil, given the different functions they perform. Nevertheless, the necessity for enhanced performance unites those AC/DC and DC/AC converters. The RC-IGBT technology facilitates an increase in the system's output current when compared with previous V-series technology or current X-series based solutions.

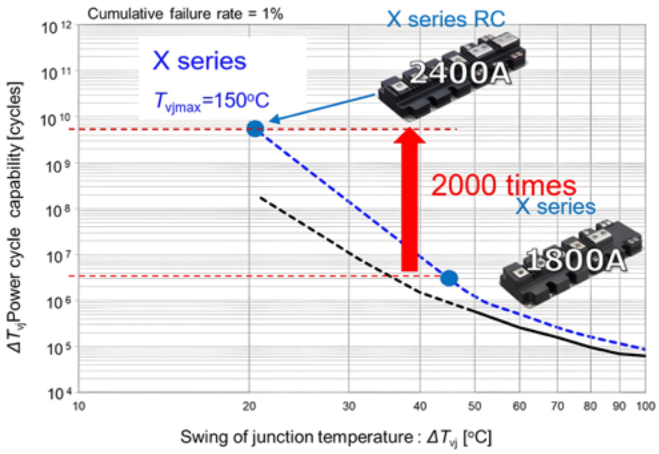

Figure 6: 1700V PrimePACK™3+ ΔTvj Power cycle life

A comparison of the operational characteristics of an 1800A and a 2400A RC-IGBT module demonstrates that the latter exhibits a longer operational lifetime. The enhanced thermal stability at identical output currents results in a strongly extended operational lifetime (Figure 6).

An additional example of the utilisation of the RC-IGBT technology, now in DualXT package, is the reduction of the system's footprint through the replacement of 2 modules of 450A Dual XT with one 1000A RC-IGBT DualXT. In addition to the reduction in the number of driver units, which facilitates control of the system, the footprint is also reduced to 40% of the initial system size. Or in case of expanding 800A based system, to deliver a power extension option, a 1000A RC-IGBT can be used (Figure 7).

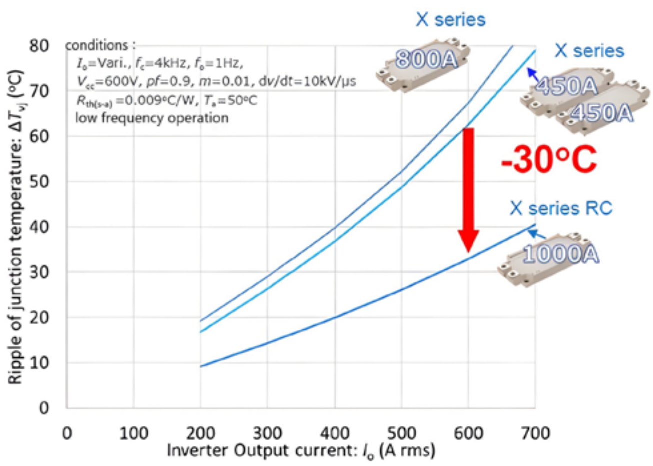

Figure 7: Calculation conditions: Io=Vari., fc=3kHz, fo=5Hz, Vcc=1200V, pf=-0.9, m=1, Standard RG, Rth(s-a)=4.7°C/kW, Rth(c-s)=1.4°C/kW(with 3W thermal grease), Ta=35°C

It is anticipated that this trend towards downsizing will become more prevalent in the future, as a result of the increased availability of a diverse range of RC-IGBT packages.

Fuji Electric's RC-IGBT product range has been designed for industrial applications and offers a maximum current rating of 2400A for modules in both the 1700V and 1200V classes for PrimePACK™3+ as well as DualXT package in 800A/1700V and 1000A/1200V variant. This represents an increase in nominal output power in comparison to the conventional X-series technology.

A comparison of the operational characteristics of two in parallel 450A or one 800A IGBT and a 1000A RC-IGBT DualXT X-series module demonstrates that the latter similar to PrimePACK™3+ RC-IGBT exhibits a longer lifetime under same operational condition. The enhanced thermal stability at identical output currents results in a markedly extended operational lifetime (Figure 8).

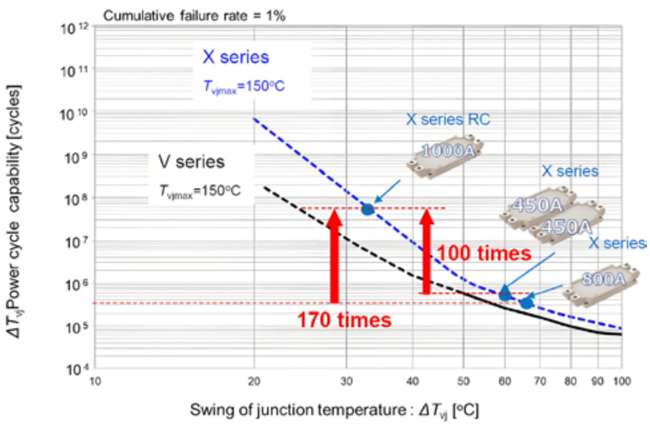

Figure 8:1200V DualXT ΔTvj Power cycle life comparison

Given the inherent challenges associated with handling currents of 2400 A, particularly in view of the generated heat in the output terminal, the PrimePACK™3+ package with two output terminals was selected as the optimal solution. The enhanced output power of RC-IGBT technology facilitates the optimisation of power conversion systems. The realisation of higher currents within the same footprint enables the ongoing miniaturisation of systems. Fuji Electric offers this technology in the PrimePACK™3+ and DualXT to meet market demands and strives to realise a safe, secure and sustainable society.

www.fujielectric-europe.com

AI server hot-plugging with robust hot-swap controllers

Strategies for reliable and continuous operation in AI server data centers using hot-swap controllers and the role of eFuses in the future

By Nitish Agarwal, Senior Application Engineer, Infineon Technologies Americas

AI servers and hot-plugging

This is the age of 24/7 AI usage where AI servers need to be always online. Their ever-growing power demand forced server architectures to transition from 12 V to 48 V, which reduced power losses by 16x, allowing greater power extraction with reduced cooling costs. An AI server rack computes the required data in an interruption-free operation and comprises multiple AI server blades operated in parallel. Server blades, in turn, are composed of a power converter, the AI processor, network switches, and a memory.

Visualize parallel AI server blades as drawers of a filing cabinet: the back of the cabinet into which these drawers (server blades) wheel in, is a 48 V live backplane, and the cabinet is the server rack. The blades are plugged into this backplane powered by the same source as the processors. If one blade fails, the load is shared by the others to keep the system running. Meanwhile, the faulty blades are replaced by plugging new blades into the live backplane without taking the entire system offline. This process is called "hot-plugging" or "hot-swapping".

To avoid costly server downtimes or high replacement costs that can run into even $9000/minute per Forbes [1], server blades must be protected against system level failures due to voltage fluctuations or thermal variations, among others. This is where hot-swap controllers come into play as reliable protection solutions for AI servers.

Hot-plugging events

Every hot-plugged server blade contains a capacitor for energy storage purposes and to filter out voltage ripple and high-frequency noise. At insertion of the server blade, the capacitor is discharged, acting as a short or low-impedance path from V_{IN} to ground. Hot-plugging a server blade in this moment creates a huge amount of inrush current for a short time. But it is strong enough to blow up the fuse or cause voltage dips in adjacent blades triggering a system shutdown. The increasing power density originating from the growing power demands of AI servers also requires additional capacitance, making it critical to reduce this inrush current.

One technique to reduce inrush current is to increase the current-path resistance by adding a series resistance between V_{IN} and C_{IN}. Increasing resistance to the power-path would cause a voltage drop, adding to I^2R losses. Another technique utilizes negative temperature coefficient (NTC) thermistors, offering a high resistance before hot-plugging. Inrush current passing through NTCs of a room-temperature server blade generates heat from I^2R losses, reducing the resistance. Thus, NTCs reduce steady-state system losses, which are significant. The resistances could be shunted using a switch/relay, which increases size, cost, and complexity. They are also unreliable when faulty blades need to be isolated.

Hot-swap controller mechanism

Clearly, a solution is needed where the input current to the capacitor can be controlled during hot-plugging without causing voltage drops or power losses during normal operations.

Imagine the backplane as an infinite water reservoir and the input capacitor as an empty water tank. To control the water flowing from the reservoir to the tank, a control valve is added, without which

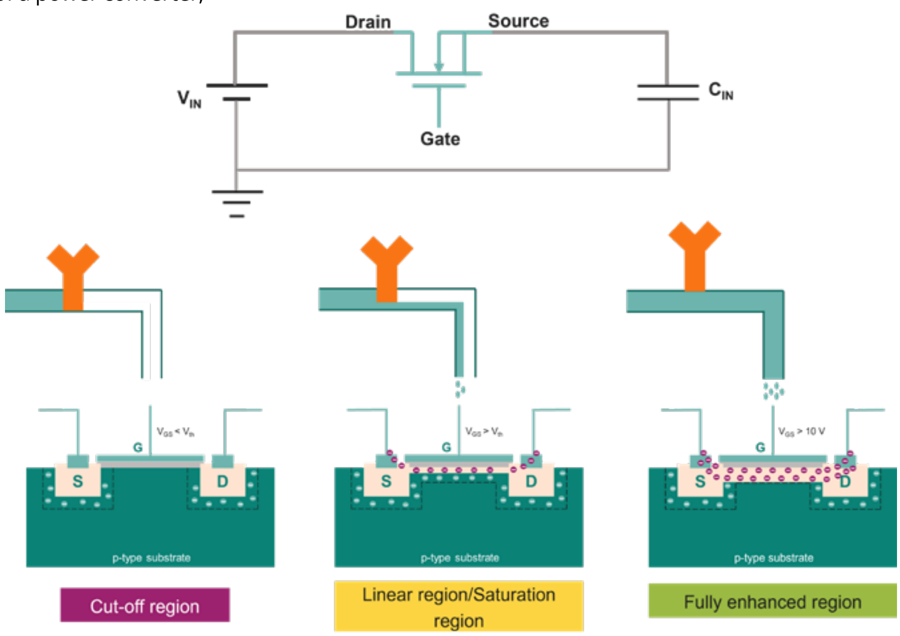

Figure 1 : Capacitor inrush current analogy with a water reservoir example

the water flows into the tank at the maximum flow rate, just like the inrush current. In this analogy, the valve is a MOSFET, whose gate voltage determines the current flowing through it. When the MOSFET gate voltage is below V_{th} (turn-on threshold), it operates in the cut-off region without allowing current to flow through, blocking the current flow (inrush current) while inserting the blade into the backplane.

As $V_{GS} > V_{TH}$, a controlled current flows through the FET. Initially, the current depends on V_{GS} while V_{DS} is high, placing the MOSFET in the saturation region, where the current is constant as long as V_{GS} is stable. As V_{GS} increases, more current flows, charging the input capacitor and lowering V_{DS}, transitioning the MOSFET into the ohmic region where the current depends on $R_{DS(on)}$.

For hot-swap applications, 100 V MOSFETs are common with typical $R_{DS(on)}$ values between 1.5 mΩ and 3.5 mΩ. Identical MOSFETs are paralleled to share current, reducing thermal stress by effectively lowering $R_{DS(on)}$ per FET.

A hot-swap controller controls the MOSFET gate voltage to regulate the capacitor current at startup. It also ensures that the MOSFET is not damaged, staying within its design limits defined by the safe operating area (SOA) curves found in the MOSFET's datasheet [2].

Infineon's five gallium nitride power semiconductor families

CoolGaN™ Transistor
- 60 V – 700 V
- 4 A – 150 A
- Broad package selection

CoolGaN™ BDS
- 40 V – 850 V
- Monolithic bidirectional switch
- Blocking voltages in both directions

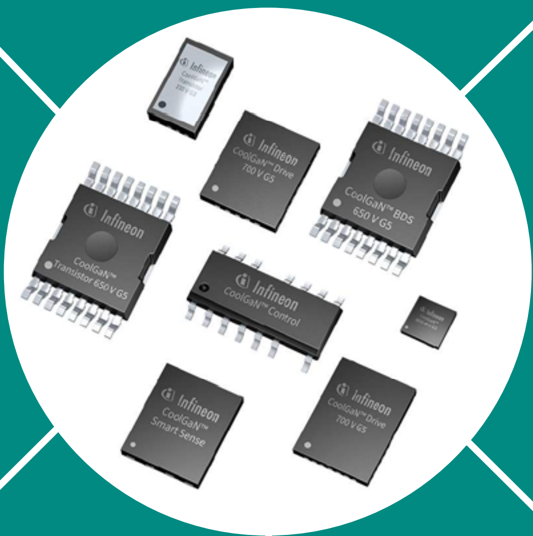

Coming soon
CoolGaN™ Smart
- 650 V – 700 V
- Current sense
- Protection features

Coming soon
CoolGaN™ Control
- Supporting multiple topologies
- System-in-package solution
- Integrated drivers

Coming soon
CoolGaN™ Drive
- 100 V – 700 V
- Integrated drivers
- Half-bridge and single switch

Find out more

Digital hot-swap controllers

To keep up with the growing power demand, digital hot-swap controllers allow for programming of the FET's SOA profiles to ensure that the FET always stays within its safe operating region, and improve overall system reliability and lifetime. Its algorithm works as follows:

1. MOSFET SOA current profile from V_{DS} = 80 V down to V_{DS} = 1 V is programmed at the desired temperature.
2. When hot-plugging, the FET's $V_{DS} = V_{IN}$. Controller refers to an internal lookup table; sets the corresponding drain current as the target FET drain current.
3. Controller ramps up V_{GS} slowly and measures current flowing through the FET, regulating it to maintain the programmed current level.
4. As current flows, the capacitor C_{IN} charges, increasing the VOUT and reducing V_{DS}.
5. Controller adjusts target regulation current as V_{DS} decreases.
6. Once C_{IN} is fully charged, the inrush event ends; controller signals power converter "Power Good".
7. Power converter powers up the processor, bringing the server blade online.

4 kW hot-swap

A 4 kW hot-swap solution with four OptiMOS™ 5 Linear FET 2 IPT017N10NM5LF2 FETs [3] and a XDP™ XDP710-002 hot-swap controller [4] is available with Infineon. The board operates from 40 V to 60 V and the nominal load current for 4000 W = 100 A; thus, four FETs are operated in parallel after thermal calculations. The SOA profile of the FET at 95°C is programmed into the controller.

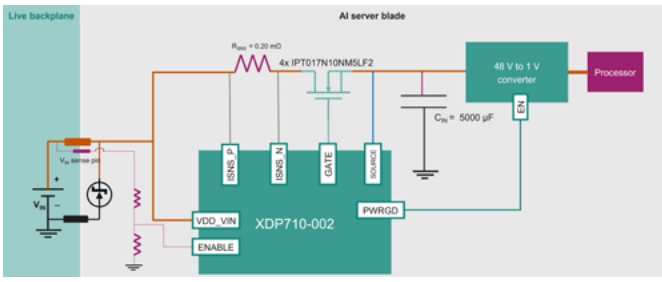

Figure 2: 4 kW hot-swap controller design

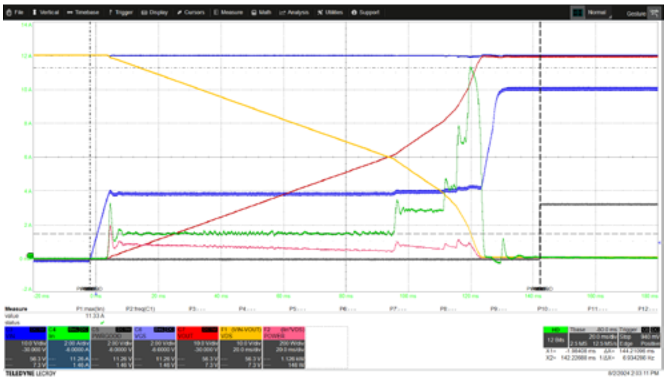

Figure 3: Typical turn-on waveforms of XDP™ XDP710-002 charging a 5000 µF capacitance

Burst mode for FET turn-on instead of continuous mode

While operating on the DC SOA line, continuous power dissipation across the FET ($V_{DS} \times I_D$) reduces reliability, especially with a larger capacitance extending the MOSFET's time in the linear region. So, the 1 ms SOA line is used, turning the FET on for 1 ms to charge the capacitor, then off to cool down, and repeating.

During turn-on, the FET charges the input capacitor without feeding the load current, and thereby stores energy. During turn-off, the controller slowly charges the capacitor while allowing the MOSFET to cool. In burst mode, the FETs operate at the 1 ms SOA line during high V_{DS} and switch to continuous mode at lower V_{DS}, providing ~9 ms (adjustable) cooling time, thus enhancing reliability.

Eliminating contact bounce during hot-plugging

The mechanical connection of hot-plugging a server blade into the backplane often causes bouncing. To prevent bouncing, the gate pulse to the inrush FET is provided only after the blade is securely plugged-in. Therefore, a voltage-sense pin can be used, which is the last to connect with the backplane and is linked to the "Enable" pin of the hot-swap controller. The controller turns on the inrush FETs only when the voltage on the "Enable" pin is above a threshold for a set duration; otherwise C_{IN} remains disconnected from the backplane.

Protecting blades and backplane during faults

The backplane must be protected against faulty blades to shield other parallel servers. Detecting faults and isolating affected server blades quickly and safely by opening the inrush FETs is of utmost importance. Additionally, external events like voltage variations/surges require protection to maintain system reliability and avoid server downtimes.

Hot-swap controllers offer protection against short-circuits, overcurrent, overvoltage, undervoltage, overtemperature, and FET faults. They isolate faulty modules without damaging the backplane and alert the system via fault pins. FETs can be latched-off, they can turn back on after self-clearing faults, or the controller can auto-retry based on settings.

Short-circuit detection is critical due to its potential catastrophic impact. Modern controllers isolate faults in <1 µs using fast comparators and strong gate pull-downs but cause high voltage spikes. TVS diodes are used to clamp these spikes, ensuring the 100 V-rated FETs handle the surge safely. Additionally, warning alerts help prevent faults with preemptive adjustments, ensuring uninterrupted supply.

Active monitoring and health reporting

The hot-swap controller's active monitoring module accessible via PMBus provides real-time accurate telemetry of voltage, current, power, temperature, and energy, with fault and warning statuses reporting. The capability to capture peaks and valleys helps identify potential fault events.

To enhance reliability and fault analysis, a black-box feature records telemetry data before, during, and after faults, allowing detailed analysis and troubleshooting.

Future trends

Rising demands seek integrated solutions like eFuses, combining linear MOSFETs, hot-swap controllers, current and temperature sensors into one package and thereby significantly reducing the size of hot-swap solutions.

eFuses offer an enhanced reliability with integrated temperature sensors providing real-time die temperature readings, shutting down the MOSFET at unsafe temperatures. Moreover, when paralleled, multiple eFuses together ensure current sharing at startup.

AI server power consumption is expected to increase to 8/12 kW, necessitating backplane voltages up to 400 V. This requires new, more robust, and reliable hot-swap controllers and MOSFETs, as failures at such high voltages could be catastrophic.

For an extensive explanation of how the hot-plugging is managed securely, read our whitepaper in the Documents section at https://www.infineon.com/xdp710-002.

References

1. Forbes: The True Cost Of Downtime (And How To Avoid It)
2. Infineon Technologies AG:
   Datasheet - OptiMOS™ 5 Linear FET 2 IPT017N10NM5LF2
3. Infineon Technologies AG:
   OptiMOS™ 5 Linear FET 2 IPT017N10NM5LF2, single N-channel Linear FET 100 V, 1.7 mΩ, 321 A in TOLL package
4. Infineon Technologies AG:
   XDP™ XDP710-002 hot-swap controller

www.infineon.com

In Pursuit of Cool: Building Better Thermal Models with Cauer and Foster Chains

When designing and analyzing power electronic circuits in simulation tools, ensuring that such systems are kept sufficiently cool requires accurate thermal models. Engineers widely use lumped-element thermal models such as Foster and Cauer chains to predict device temperatures and heat flow. While these chains look simple, they have subtle complexities that can undermine model accuracy and thermal behavior. Here, we dive into how to get the most out of these models – from measuring impedance curves to best practices for building better, more reliable thermal models.

By Alexander Weyman, Plexim

With the demand for ever-greater efficiency and reliability in power electronics, the need for accurate thermal models in simulation software is of critical importance to improve thermal management. With growing computing power, high-resolution thermal FEM models of single devices are becoming increasingly feasible, enabling engineers to capture detailed thermal behavior and optimize cooling. However, such model complexity can hinder simulations at the system level, making efficient, performance-optimized models the preferred choice. In this field, thermal circuit models, especially chain-like networks of the Cauer and Foster type, have established themselves as a standard and powerful tool for modeling heat transfer dynamics and semiconductor junction temperatures. Despite their simple structure, these models are prone to typical pitfalls, often rooted in a misunderstanding of the basic principles behind Cauer and Foster chains.

Understanding Cauer and Foster Thermal Chain Models

A chain-like circuit of the Cauer type is closely related to a physical representation of a thermal system. Derived from discretizing the one-dimensional heat equation, Cauer chains model the thermal path as a network of thermal resistances (R_{th}) and thermal capacitances (C_{th}). From this perspective, it becomes clear why each R-C pair in a Cauer chain can be thought of as representing a physical layer within the device. This direct correlation allows intuitive adjustment of the model based on material properties and geometric dimensions. For example, in a power semiconductor device, the heat generated at the junction must pass through several layers before dissipating into the ambient environment. By representing each layer with an R-C pair, the Cauer thermal chain captures the heat flow dynamics accordingly. Choosing more or fewer R-C pairs adjusts the resolution at which the one-dimensional heat path is discretized, allowing a balance between model complexity and the desired level of detail.

In contrast, Foster type thermal chains offer an abstract approach to modeling temperature response, where individual R-C pairs are not related to the physical layers. Instead, the entire set of R-C pairs collectively represents the full thermal path, terminating at a constant temperature. There is a clear mathematical procedure for transforming a set of Foster R_{th} and C_{th} values into a corresponding set of Cauer R_{th} and C_{th} values, and vice versa, with flexibility in the arrangement of the Foster R-C pairs. As visualized in Figure 1, Foster chains lack a direct connection to the physical heat equation but, despite their abstract nature, they are widely used in practice because of their mathematical simplicity in describing thermal response to a step change in power input. This simplicity allows Foster R_{th} and C_{th} values to be extracted through curve fitting of the measured transient thermal impedance Z_{th} curve. Yet, common pitfalls in measuring the Z_{th} curve and obtaining suitable Foster R_{th} and C_{th} values from it are not always easy to spot. Here, we highlight a few key challenges and present solutions.

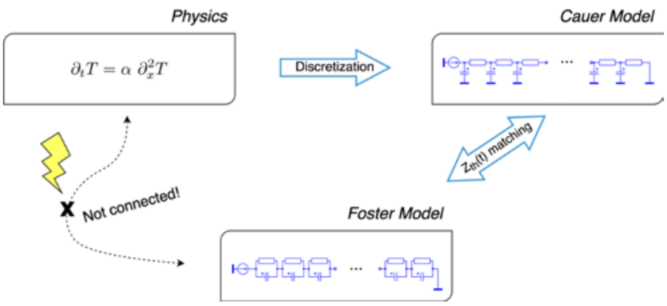

Figure 1: Relationships between the Cauer model, the Foster model, and the physical perspective on describing thermal paths.

Common Pitfalls in Measurement and Application

Analogous to electrical resistance, defined by Ohm's law as the ratio of voltage across a resistor to the current flowing through it, R=U/I, thermal resistance can be characterized by the temperature difference across a thermal resistor relative to the heat flow passing through it, R_{th}=ΔT/P. For the transient case, it may then seem intuitive to treat individual parts of a thermal path as single resistor-like entities, that is, as one-port networks. This would imply, however,

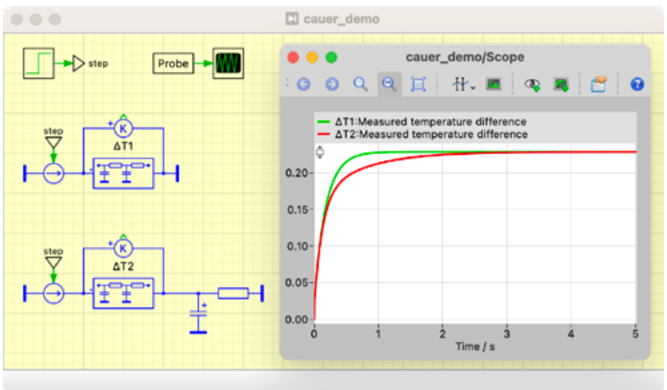

Figure 2: A simple PLECS model demonstrating how identical thermal paths, represented as Cauer chains, show different thermal behavior depending on how the path is continued.

that the division $Z_{th}(t)=\Delta T(t)/P$ results in a unique transient thermal impedance curve for the thermal path in question. Unfortunately, this is not the case. In fact, the shape of the $Z_{th}(t)$ curve can vary significantly depending on how the reference temperature at the end of the thermal path changes during the measurement. Figure 2 illustrates how $\Delta T(t)$ differs for two identical physical thermal paths represented as Cauer chains, depending on how the path is continued. Since Cauer chains are internally connected to a thermal ground, they go beyond the concept of a simple one-port network.

Foster chains, in turn, are one-port networks that produce two identical temperature profiles when used in place of the Cauer chains shown in Figure 2. Foster chains should not be connected in series, as this fails to accurately capture the physics of thermal heat flow along the path, resulting in a flawed model for representing thermal behavior. Recognizing that Foster chains must represent the entire thermal path, rather than individual segments, highlights the importance of maintaining a constant temperature at the end of the path when measuring $Z_{th}(t)$ curves. While this may seem less intuitive, the 'entire path' can also refer, for instance, to a junction-to-case path – as long as the temperature at the case is kept constant during measurement. Such a measured curve between junction and case can then serve as the basis for deriving Cauer R-C parameters through a well-fitted Foster model. This resulting Cauer chain, with its close relation to the physical heat equation, can then be incorporated into a larger Cauer model that extends, for example, from the junction to the ambient environment. This avoids the series connection of Foster chains which is incorrect as described previously. Next, we dive into what it means to obtain a 'well-fitted' Foster model.

Subtleties in the Curve Fitting Process

The simplicity with which the Foster model describes $Z_{th}(t)$ also brings with it certain common pitfalls in the curve-fitting process. Given the mathematical function used to fit the Foster model to an impedance curve, $Z_{th}(t)=\Sigma_i R_i (1 - e^{-t/\tau i})$, with time constants $\tau_i=R_iC_i$, it becomes evident that a single term in the sum can be split into two separate contributions with the same τ value without changing the shape of the curve. This subtlety can cause the curve-fitting algorithm to return multiple τ values that are very close to each other. In practice, this can become problematic when Foster parameters are provided for a thermal path intended for inclusion in an extended thermal network, such as junction-to-case Foster parameters. When these parameters are converted to a Cauer model for integration into a larger path, unrealistically large thermal capacitances can result, significantly impacting the modeled heat flow and, consequently, the predicted junction temperature. One example is shown in Table 1, taken from an official datasheet of an IGBT device. Due to closeness of the τ_3 and τ_4 values, the derived Cauer parameters result in a total thermal capacitance of 25 MJ/K – equivalent to around 65 tonnes of copper – thereby significantly delaying heat flow from junction to case.

i	1	2	3	4
r_i [K/W]	0.0039	0.04368	0.03203	0.00789
τ_i [s]	8.56E-4	0.0279	0.0913	0.0914

Table 1: Example Foster parameters for $Z_{th,JC}$ with close τ_3 and τ_4 values, provided in an IGBT device datasheet.

Another subtlety that arises from the $Z_{th}(t)$ fit function from the Foster model is that an additional R-C layer with a large τ and a small R can be added to the Foster chain without noticeably changing the shape of the $Z_{th}(t)$ curve. However, if the curve-fitting algorithm introduces an additional Foster layer in this way, it can lead to unrealistically large thermal capacitances when converted to a Cauer model, potentially causing a substantial delay in heat flow.

PLECS has a solution to avoid these subtle pitfalls when fitting a Foster model. With the release of PLECS version 4.9, we have introduced an algorithm that automatically detects these issues and offers users the option to fix them with the click of a button. Figures 3a and 3b demonstrate how PLECS detects both issues in the shown example Foster parameters from an official datasheet and provides a fix.

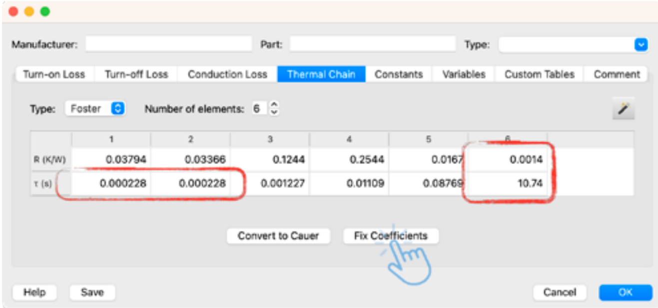

Figure 3a: The new 'Fix Coefficients' feature in PLECS 4.9 automatically detects issues in Foster model parameters, highlighted in red.

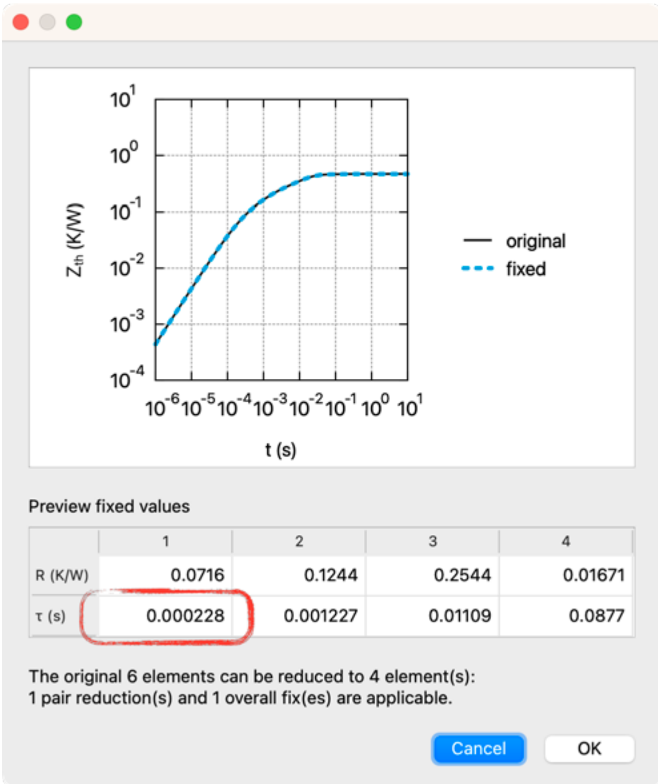

Figure 3b: Preview of the fixed values displayed in a separate window.

The Next Level: Modeling Thermal Crosstalk

Building on the foundation of thermal chains, engineers have developed sophisticated networks to model more complex behavior such as thermal crosstalk, where the heating of one chip affects the temperatures of neighboring chips. It is important to remember that this approach, which uses arbitrarily branched thermal chain networks, is valid only when assuming effective one-dimensional heat flow along the physical paths. Additionally, isolated measurement of these paths, with reference temperatures needing to be kept constant, is necessary to determine accurate R-C values for the chains. Given the practical challenges in achieving these conditions, we present a more accessible approach to modeling thermal cross-coupling using thermal chains.

Following a similar approach as with the choice between the physically-based Cauer model and the more abstract but useful Foster model, we aim for a black-box approach to thermal crosstalk, capturing thermal interactions without detailing the physical mechanisms by which nearby heat sources influence each other. Assuming that contributions from heat sources can be separated, we can ask how a unit step change in power applied at one chip affects the transient temperature increase at another. This approach naturally leads to the mathematical description of a thermal impedance matrix, where each matrix element provides the exact answer to this question. Moreover, this convenient matrix description allows

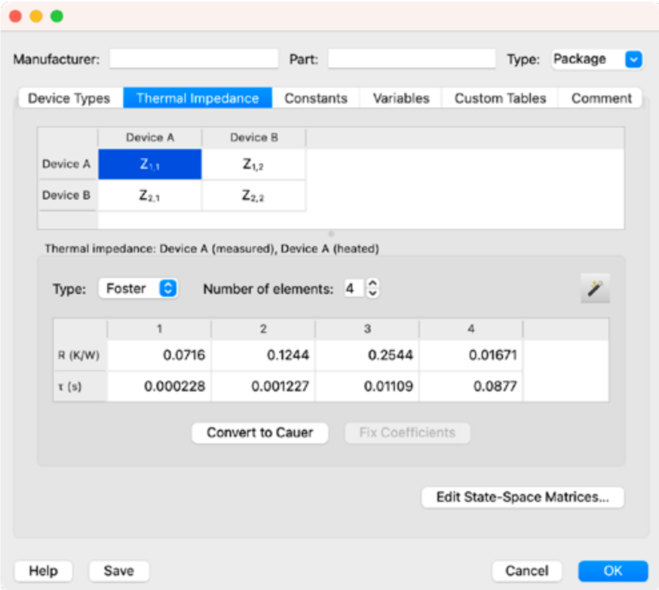

Figure 4: Since PLECS 4.8, the Thermal Package Description option allows users to define a thermal impedance matrix, enabling the modeling of thermal crosstalk through the off-diagonal matrix elements.

for the direct and straightforward measurement of each transient thermal impedance matrix element.

While the concept of using thermal impedance matrices is not new in thermal modeling, a key challenge is to accurately account not only for the correct temperature behavior but also for the correct heat flow leaving a thermally coupled system, so the thermal path can be extended in a physically meaningful way. In PLECS, we address this challenge by embedding Cauer chains within a state-space representation derived from a user-defined impedance matrix. The way in which the state-space representation is constructed ensures that the heat flows measured individually from each device are accurately recovered. Figure 4 shows how the thermal impedance matrix is integrated into PLECS within the Thermal Package Description window. By clicking on individual matrix elements, users can provide Foster or Cauer parameters to define each $Z_{i,j}(t)$ element.

Conclusion

Despite – or precisely because of – their simplicity, thermal Foster and Cauer models are widely used as highly efficient tools for analyzing the thermal behavior of power electronic systems. Understanding the physical basis of the Cauer model and the abstract nature of the Foster model is invaluable for avoiding common pitfalls in measurement, curve fitting, and integration of thermal models. Recent advancements in PLECS include inbuilt mechanisms to detect common issues in modeling thermal circuits, support the development of more reliable models, and greatly simplify the modeling of thermal crosstalk. The pursuit of cool, after all, is about more than just managing heat – it is about using these models to improve reliability and performance, setting new standards for innovation in power electronics.

www.plexim.com

The Power Module that Stabilizes the Grid

In modern power grid systems, maintaining a stable grid frequency is more important than ever due to new challenges, such as the transition to renewable energies. This is largely due to the significant amount of energy consumed in today's world and governmental goals to reduce carbon emissions. Consequently, the demand for energy storage devices is growing. A crucial element of an effective Energy Storage System (ESS) is the Power Conversion System (PCS). The PCS acts as an interface between the direct current (DC) batteries and the electrical grid.

By Patrick Baginski, Sr. Field Application Engineer, Vincotech

A power Conversion System (see Figure 1) is equipped with a power semiconductor module as its main component, which connects the energy storage battery system to the power grid to enable bidirectional conversion of electrical energy. When there is excessive power generation, the PCS charges the batteries. If the grid requires additional energy, the PCS supplies the stored energy. Additionally, it provides inertia energy to maintain the grid frequency close to 50/60 Hz. This can be achieved with a mechanical solution like a flywheel, which stores energy by spinning a mass with a moment of inertia. These energy storage systems are typically large and heavy but can release a high amount of energy in a short time. Such systems can reach up to 100+ kW, and more units can be connected in parallel if more power is needed.

A more modern solution is battery storage systems, also known as Energy Storage Systems (ESS), with the PCS as the main component for energy conversion. Any type of battery can be used, but Lithium-Ion batteries are preferred due to their higher power density and longer lifespan compared to lead-acid batteries. Since megawatts of power are required, these systems can be built from several smaller units or a single large one. This article discusses a specially designed product intended for use in high-power systems.

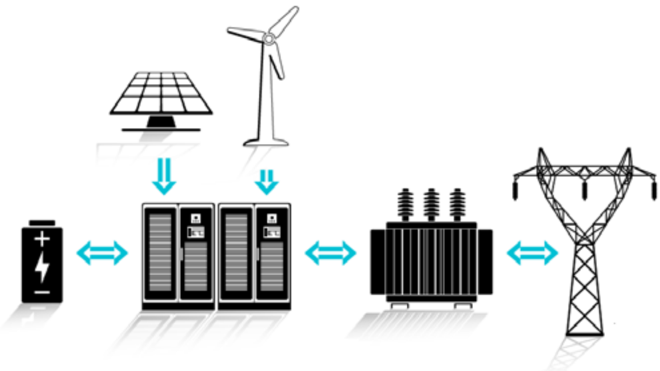

Figure 1: Power conversion system

A stable grid frequency around 50/60 Hz is necessary for the correct operation of many devices. This is especially true for older devices that generate their internal operating frequencies and timings from the grid frequency. However, modern devices use DC/DC power supplies and generate frequencies from internal oscillators or receive synchronization signals from servers.

VINcoX - 3-level high power module

VINcoX modules are specifically designed for UPS and ESS applications ranging from 160 kW to 1.4 MW, depending on operating conditions. These modules are optimized for bidirectional operation. Essentially, it is a platform consisting of up to three power modules connected by a high-power PCB. All main potentials are shared on the PCB, resulting in decreased stray inductance.

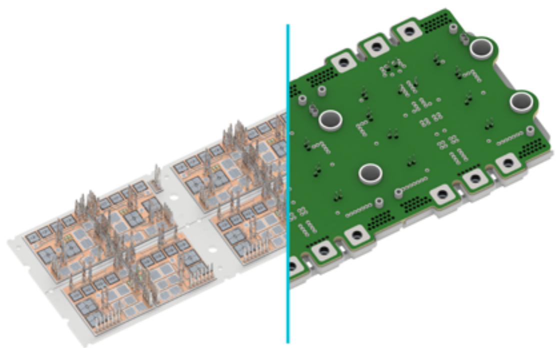

Figure 2: VINcoX12 power module

Currently, two different topologies are available: a 3-level T-type topology with 1200 V and 650 V components for 1000 V systems, which can be provided with snubber capacitors as an option, and an I-type topology with 1200 V components for DC-links exceeding 1500 V. Switching frequencies are relatively low in this power range, so semiconductors with low conduction loss are used —in this case, the Mitsubishi M7 technology. Alongside a low VCEsat, it also offers superior H3TRB capability compared to other vendors.

A symmetrical layout is the key

A challenge with larger power modules is that many semiconductors need to be switched in parallel. All devices should switch simultaneously to achieve good current sharing. Long connections inside the power module could result in turn-on and turn-off delays, causing uneven loads on chips. Therefore, each of the three segments has its own gate-emitter connections. Furthermore, each commutation loop on the DCB has its own connections. The driver PCB, which can be pressed or soldered to the press-fit pins, needs to manage these signals. Design hints and layout recommendations are provided in the evaluation driver board documentation.

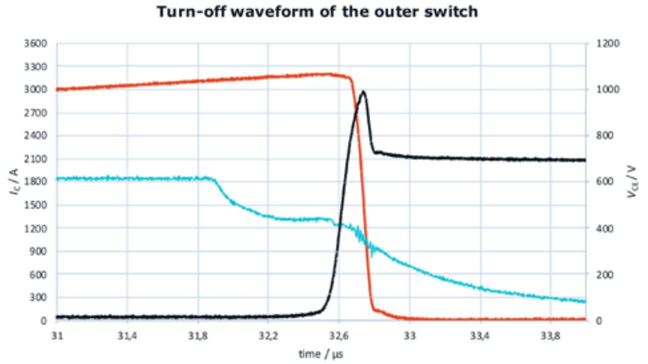

Figure 3: Turn-off waveform of an 1800 A module @ IC = 3200 A at ambient temperature

The turn-off waveform in Figure 3 is measured with the largest available VINcoX12 module, featuring a nominal chip current of 1800 A (model 70-W624NIA1K8M701-LD00FP70). This module has 100% rated components in all positions, making it an ideal choice for 4Q operation. As shown, the module has very low stray inductance and can be switched quite aggressively with a 0.5 Ω gate resistor, resulting in an overvoltage spike of only 41%, which is approximately 990 V for a 1200 V semiconductor.

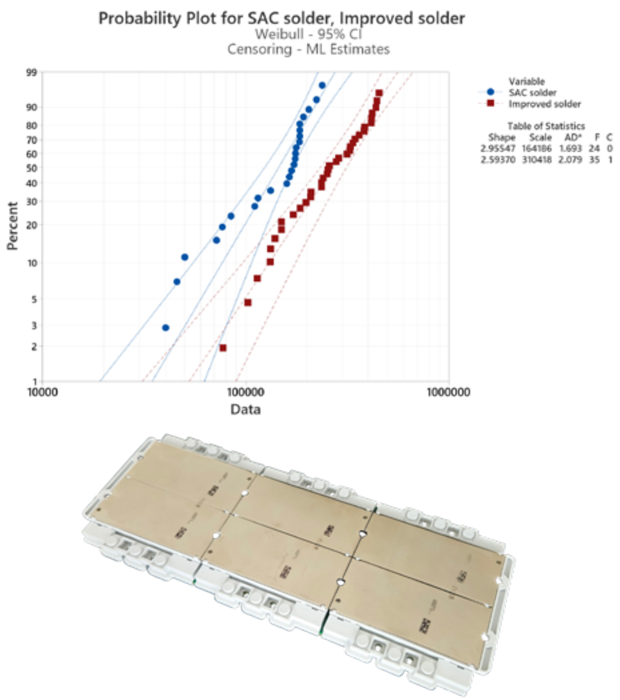

Figure 4: PCs capability and VINcoX12 backside

Reliability has high priority

Reliability is critical for many applications, so this module does not use a single large copper baseplate but instead has two baseplates per segment (see Figure 4). This design means a VINcoX12 module consists of six baseplates. These are decoupled from each other, resulting in less absolute thermal expansion compared to a single baseplate, which reduces mechanical stress on the thermal interface material.

For many applications, thermal reliability is of particular interest. Heavy load changes stress the chip/bond wire connections and the solder material between the chip and DCB. Additionally, operating at high loads and high chip temperatures may degrade the chip solder material if it becomes too hot. The new advanced solder material contributes to both, resulting in a significantly longer lifetime. It enhances the power cycling capability by nearly two times and the high-temperature forward bias capability by up to nine times.

High reliability and high efficiency with VINcoX modules

VINcoX modules are specifically designed for 3-level high-power applications, primarily for energy storage systems to provide inertia energy. With 100% rated components in all positions, they are ideal for applications requiring bidirectional operation. The flexibility to add up to three segments allows for coverage of chip current ratings between 400 A and 2400 A. T-type and I-type topologies are available for both 1000 V and 1500 V systems. The blocking voltage capability of the I-type topology with 1200 V components allows for even higher DC-link voltages. High reliability and long lifespan are achieved by using two separate baseplates per segment and advanced solder material for superior power cycling and high-voltage forward bias capability. As an option, modules can be delivered with pre-applied phase-change material to eliminate the thermal pasting process in the customer's production area. Overall, the VINcoX platform is suitable for all 3-level applications ranging from 200 kW to 1.5 MW.

www.vincotech.com

Kilowatt DC/DC Converters for Fuel Cell Solutions

Fuel cells are electrochemical devices that convert the chemical energy from a gaseous fuel, often hydrogen, directly into electrical energy. This process occurs in a reaction chamber, or "cell" (Figure 1). When hydrogen serves as the fuel, the process resembles electrolysis in reverse.

By Steve Roberts, Innovation Manager, RECOM Power

In electrolysis, electricity splits water into hydrogen and oxygen, producing hydrogen at the cathode and oxygen at the anode in a 2:1 ratio (H_2O). Conversely, hydrogen combines with oxygen (from air or pure sources) in a hydrogen fuel cell to produce an electrical current, with water and heat as the only by-products.

While fuel cell technology is often viewed as being modern, it dates back to the first prototypes built by the scientists Sir Humphrey Davy and Sir William Grove in the early 19th century. In the 1960s, practical hydrogen fuel cell technologies were developed to power welding equipment, agricultural tractors, and even space missions. A significant hurdle to their further development was designing durable interface technology to separate the gases from the liquid electrolyte in the cell. The interface needed to be gas-permeable, electrically conductive, and resistant to both electrolyte corrosion and the heat generated. Today, constructions using proton exchange membranes (PEM) have largely addressed these issues, making stacked fuel cells a viable option for clean, efficient power across multiple sectors like transportation and residential energy.

Fuel cells are an increasingly attractive option in transportation, offering an alternative to fossil fuels and helping reduce greenhouse gas emissions. Fuel Cell Electric Vehicles (FCEVs) powered by hydrogen are now being produced by many major automakers, such as BMW, Toyota, Honda, and Hyundai. FCEVs offer certain advantages over Battery Electric Vehicles (BEVs), particularly for long-distance travel, due to quicker refueling and greater range potential.

High-pressure hydrogen refueling stations operate similarly to traditional fuel pumps, whereas BEVs often require lengthy charging stops or larger, heavier batteries. This makes fuel cells ideal for applications in long-haul trucking, buses, and other heavy-duty transport, where rapid refueling, lighter weight, and extended range are key factors. As a result, FCEVs are increasingly focused on trucking and railway applications, while clean fuel cell-

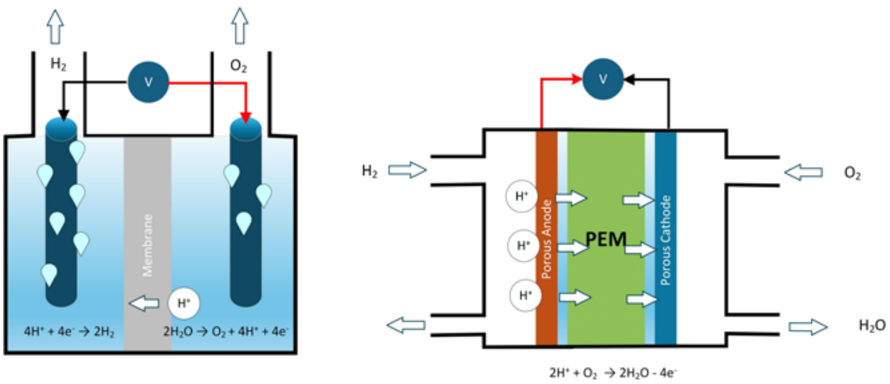

Figure 1: Electrolysis Cell vs Fuel Cell Schematic

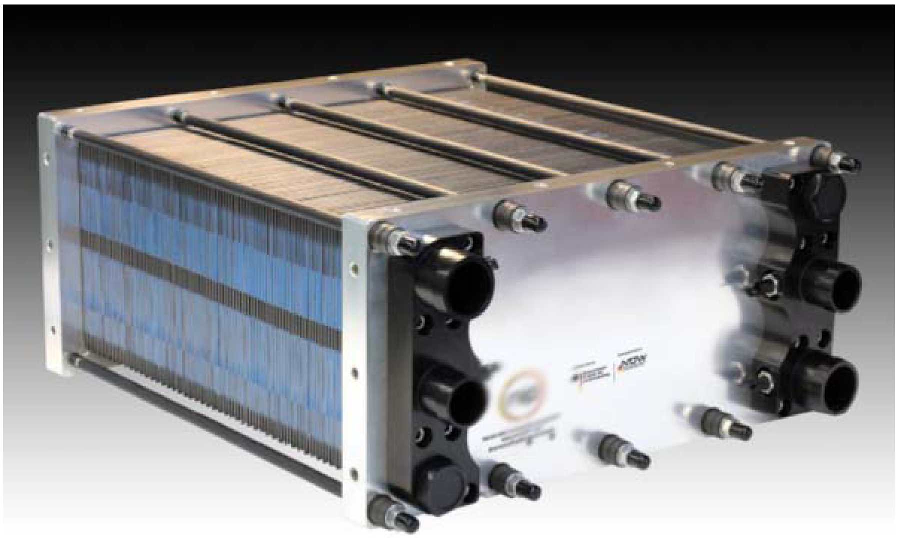

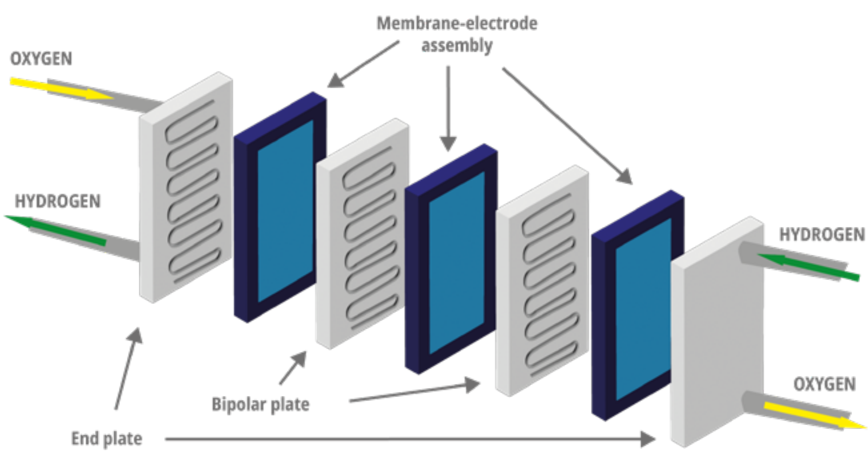

Figure 2: Fuel cell stack construction

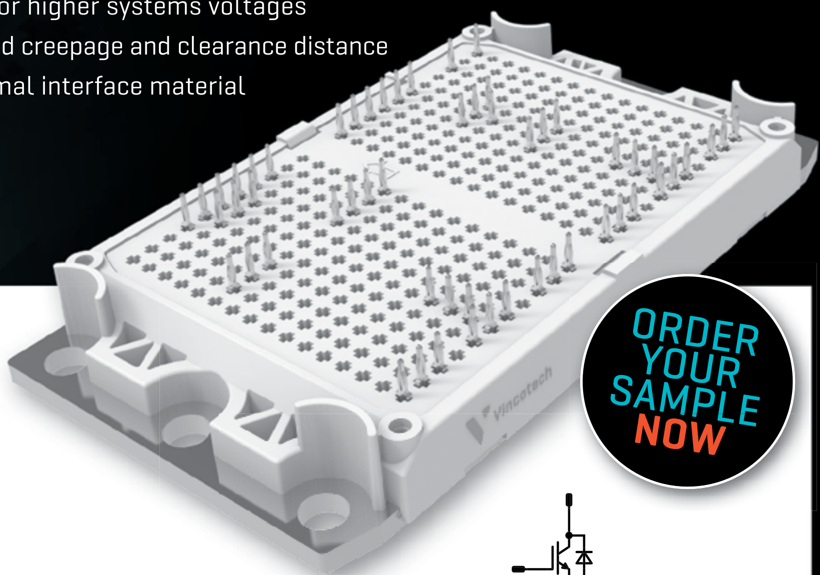

ORDER YOUR SAMPLE NOW

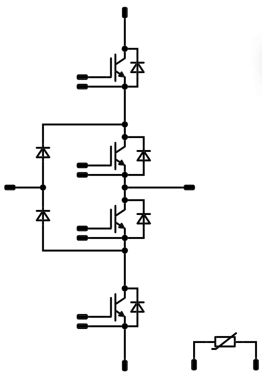

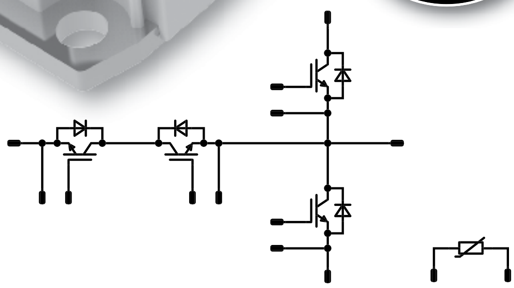

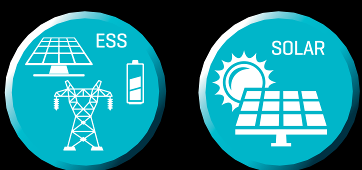

ESS
SOLAR

powered buses and trams can already be found in many urban areas. Additionally, small scale FC units can be easily retrofitted to refrigerated containers and trailers, avoiding the need to have a continuously running diesel engines to keep perishable goods cold.

Hydrogen fuel cells are also being applied in stationary power systems, powering buildings, industrial sites, and even entire communities. Fuel cells are inherently scalable: adding more cells increases voltage, expanding cell surface area increases current, and connecting multiple stacks in parallel boosts power. However, as individual cells generate relatively low voltages (0.5-0.8V), fuel cells are typically stacked together to deliver useful output voltages of 200V-300V with high current (hundreds of amps) to simplify the construction (figure 2).

Portable power applications are another promising use for fuel cells, particularly in the military, medical, and consumer electronics fields. Fuel cells provide longer operational times than traditional batteries, an advantage in remote, off-grid, or emergency situations. The U.S. military, for example, is exploring small-scale fuel cells to power field equipment, reducing soldiers› dependence on heavy battery packs.

Despite recent advances, fuel cell energy still faces inherent technical challenges that hinder widespread adoption. Addressing these challenges is essential for hydrogen fuel cells to play a significant role in our energy transition.

The Reaction Time Problem

Since fuel cells generate power through a chemical reaction involving two gases, there's a delay between gas supply and power output as the fuel permeates through the stack (Figure 3). For fixed stationary applications, this delay is manageable. However, for hydrogen fuel cell vehicles, even a brief reaction delay is unacceptable, so fuel cell-powered vehicles also use high-voltage (HV) batteries for immediate power and acceleration. These HV batteries can, however, be relatively small as they are continually recharged by the fuel cell stack.

Another challenge is an emergency stop. Unlike fuel-burning engines that can be quickly turned off, fuel cells need to be flushed out to remove the reaction gases to stop producing power. This makes shutdown a relatively slow process.

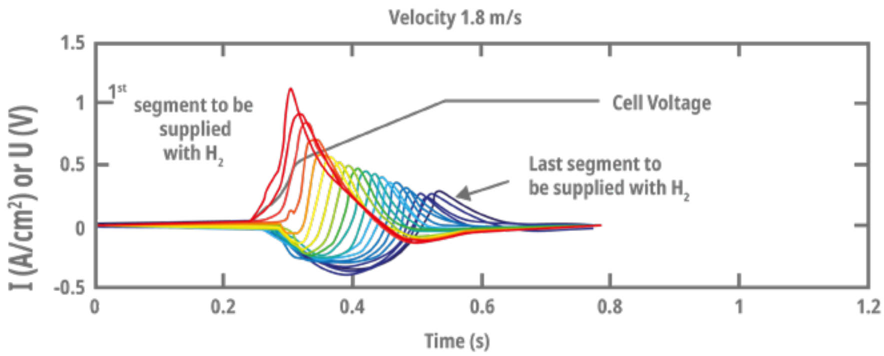

Figure 3: Fuel Cell Stack Reaction Time (Source: LEMTA - University of Lorraine)

Figure 4: RECOM's Modular 5x15kW (75kW) Fuel Cell DC-DC Converter

The Role of DC/DC Converters in Fuel Cell Systems

DC/DC converters address both the reaction delay and shutdown issues while managing the interface between the fuel cell and battery pack.

They:

- Act as boost converters, converting the fuel cell's low-voltage, high-current output to a higher-voltage, lower-current battery charging output.
- Stabilize the startup and shutdown ramps and mitigate any load transients, providing the stable charging voltage required by the battery pack.
- Track the fuel cell's maximum power point (MPP), adjusting it based on load, time, and temperature to maintain optimal efficiency.
- Disconnect the fuel cell stack abruptly in emergencies.
- Monitor battery voltage and current, preventing overcharging or deep discharge, and safely handling any battery faults.
- Integrate with the vehicle's CAN-bus communication system for centralized monitoring and control.

The modular 15kW DC/DC solution from RECOM offers up to 75kW by connecting five modules in parallel, making it suitable for heavy-duty applications like trucks, marine vessels, railway rolling stock, and high-power off-grid EV charging stations. This converter has a nominal 150VDC input, but it operates across a 46 to 275VDC range with peak efficiency of around 94%. The output voltage can be set between 200V and 800V to match the traction battery, with a maximum input current of 500A and a maximum output current from 85A to 220A. An onboard microcontroller manages input and output voltage monitoring to within ±2% of the set voltage and ±5% of the set current. The solution is also shock and vibration ECER100 conform, while integrated ECER10 EMC filters allow for drop-in installation in automotive applications.

L iquid cooling enables a compact design and wide operating temperatures, with the 75kW unit measuring just 750 x 400 x 200mm. The DC/DC converter operates at full power between -40°C and +50°C ambient temperatures, with built-in short circuit, output overcurrent, output overvoltage

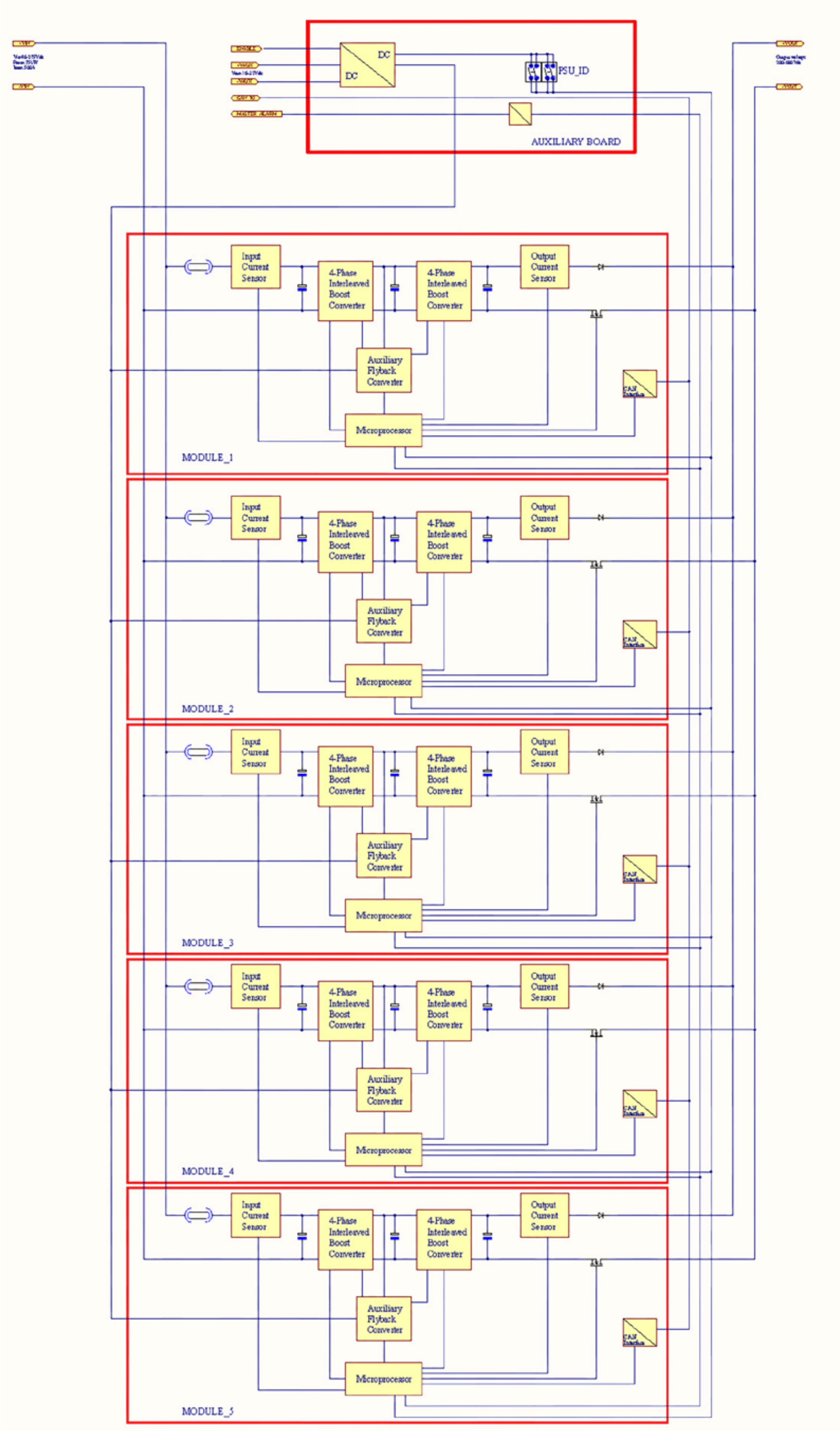

Figure 5: Modular 75kW DC/DC Converter

protection, and automatic shutdown if the cooling system fails.

Each 15kW module employs a two-stage, four-phase interleaved boost converter, allowing efficient operation across a wide range of input and output voltages. Digital control ensures accurate monitoring of all currents and voltages, maintaining peak performance under all load conditions and ensuring a rapid response to any faults.

The architecture is modular and versatile, allowing for optimization for different output voltages or power requirements from 15kW up to 75kW. Parallel connections between units also allows scaling, enabling configurations up to 225kW, ideal for high-power off-grid BEV chargers.

The J1939 CAN-Bus interface connector provides a wired emergency shutdown and alarm signal as well as the digital interface.

Conclusion

Fuel cells offer a versatile and promising pathway toward a cleaner, more sustainable energy landscape representing a crucial step toward the decarbonization goals required to address climate change. When paired with programmable kilowatt DC/DC converters, fuel cells offer practical solutions to sectors that are hard to electrify, and hydrogen fuel cell vehicles can help reduce our over-reliance on BEVs and excessive stress on the electrical grid.

www.recom-power.com

High-Efficiency Class E RF Generators using GaN FETs

A novel circuit topology has been developed for applications requiring high-voltage RF energy. It uses an unusual combination of an RC-based oscillator, a GaN FET and driver to deliver RF power at efficiencies over 95%.

By Tolga Aydemir, principal electronics consultant at 42 Technology

Advances in radio frequency (RF) generation have led to innovative designs transforming applications within the sub-100 MHz region. Among these, high-efficiency self-oscillating Class E RF generators stand out for their simplicity, robustness, and remarkable performance by leveraging Gallium Nitride (GaN) transistors. These generators can achieve efficiencies over 95% with output voltages of several kV from a few watts up to 1 kW depending on the application.

Self-oscillating Class E generators are ideal for generating high-voltage RF signals efficiently in applications where precise oscillation frequency is less critical, as they eliminate the need for external signal sources or strict frequency controls. Self-oscillating designs also benefit from automatically tuning to minor variations in resonant tank circuit parameters, making them resilient to component tolerances and environmental variations. By implementing self-oscillation in a GaN-enabled Class E driver stage, along with GaN drivers, this design further enhances efficiency due to the superior switching characteristics of GaN devices. Additionally, a kick-start circuit increases reliability by ensuring the oscillation initiates correctly upon power-up.

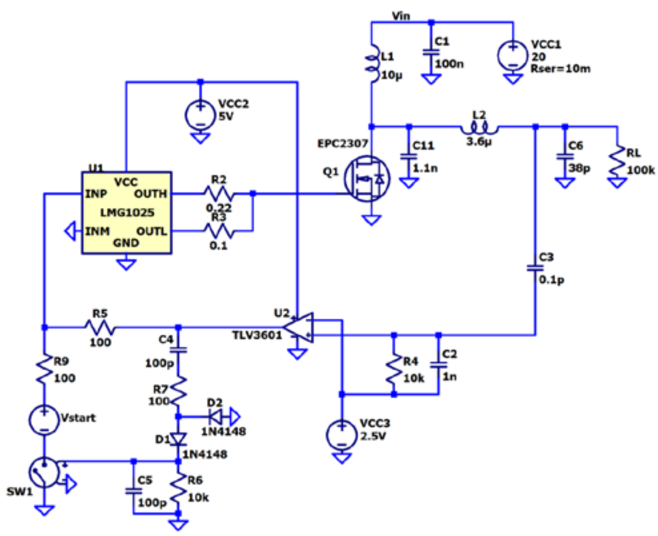

Figure 1: Self-oscillating Class E generator operating at 13.56 MHz.

Design and operation

Figure 1 shows a self-oscillating Class E generator operating at 13.56 MHz. This design leverages GaN FETs to achieve over 95% efficiency while generating output voltages of several kV, making it suitable for use in applications such as dielectric heating, ion traps, and RF lasers used within industrial, scientific research and medical sectors.

Initial start-up and oscillation

When the circuit is first powered on, Vstart provides the initial signal to kick-start the oscillation process. Vstart is an oscillator running at a frequency close to the intended operating frequency of the Class E stage (13.56 MHz). Its output is coupled through resistor R9 into the input of the gate driver U1 (LMG1025).

The gate driver drives the gate of Q1 (EPC2307 GaN FET), causing it to start switching at the Vstart frequency. As Q1 switches on and off, it drives the resonant tank circuit formed by L2 and C6. C11 acts as the shunt capacitor typical in a Class E configuration, shaping the voltage waveform. The tank circuit builds up energy, and the AC voltage amplitude at the node connecting L2, C6, RL, and C3 increases, producing an almost sinusoidal waveform.

Feedback and self-oscillation mechanism

The AC signal from the tank circuit is picked up by capacitor C3 and fed into the positive input of the comparator U2 (TLV3601). Resistor R4 and capacitor C2 form a voltage divider and provide a DC bias. The negative input of the comparator is connected to a DC reference voltage (VCC3).

When the AC amplitude is sufficient, U2 toggles its output in phase with the AC signal, following the initial Vstart frequency. The comparator's output charges the peak detector circuit composed of C4, R7, D1, D2, R6, and C5. Once the voltage across C5 reaches a threshold (e.g., 1 V), it triggers SW1 to stop the Vstart signal, allowing the circuit to enter self-oscillation mode.

Self-oscillation and steady-state operation

In self-oscillation mode, U2 continues to drive U1 using feedback from the resonant tank circuit. The self-oscillation frequency is determined primarily by L2 and C6, settling at approximately 13.56 MHz in this particular design. The circuit is carefully tuned to stay within the Class E operating region, ensuring high efficiency by minimising the overlap between voltage and current during Q1's switching.

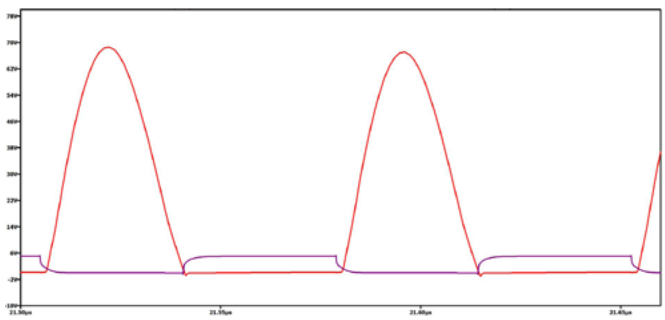

Figure 2: Drain and gate voltage waveforms confirm Class E operation.

Performance insights

Figures 2 and 3 provide further insights. Figure 2 shows the drain and gate voltage waveforms of the GaN FET, confirming Class E operation as the FET switches on when the drain voltage reaches zero, minimising power dissipation during transitions. Figure 3 illustrates the amplitude build-up on the load after powering the circuit, demonstrating efficient energy transfer and rapid attainment of steady-state oscillations.

Output voltage and efficiency

At the optimal operating point, the output voltage across RL is approximately 2.75 kV RMS, with a power dissipation of 75.5 W on RL. The simulated efficiency is over 95%. However, the measured efficiency in practical implementations tends to be slightly lower


Sanan - Your Partner for
Wide Band Gap Solutions
SiC Mundus Creatus Est
Power SiC MOS FETs
Power SiC SBDs
Power SiC & GaN foundry services
Full turnkey manufacturing platform
www.sanan-semiconductor.com/en
Europe sales.europe@sanan-ic.com
Hong Kong sales.hk@sanan-e.com
Japan sales@sanan-jt.com
Americas sanan-semi@luminus.com
San'an

because of factors such as component imperfections, parasitic elements and additional circuit losses not accounted for in the simulation. With further tuning and optimisation, this circuit can be adapted for dielectric heating, ion traps or RF laser applications.

Managing component drift and load variations

The high-Q resonant tank circuit is sensitive to minor variations in components L2 and C6, affecting output amplitude and efficiency; and load deviations from the target (e.g., 100 kΩ) can also lead to reduced efficiency and potential overheating of the GaN FET.

Auto-tuning techniques, such as using voltage-controlled tunable capacitance in the shunt and tank capacitors via MOSFETs, are able to address these issues. Adaptive control mechanisms can adjust circuit parameters in real-time to help maintain optimal performance despite component drift or load changes.

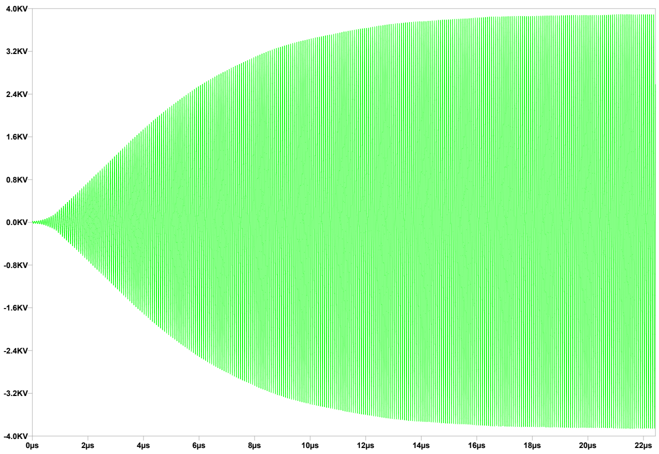

Figure 3: Amplitude build up on the load after powering the circuit.

Transforming industries with RF power

Innovations in self-oscillating Class E RF generators are part of a broader trend impacting various fields within the sub-100 MHz region. For example, RF energy powers dielectric heating for drying and curing plastics and for cooking food, and to power RF lasers (e.g, CO_2) for precision cutting, welding and engraving. Semiconductor fabrication uses RF-powered plasma to etch and deposit materials at micro and nano scales. RF systems are also indispensable in particle accelerators, mass spectrometry ion traps, and in medical treatments such as RF ablation to destroy cancerous cells or to correct heart arrhythmias through minimally-invasive procedures.

Solid-state RF and non-linear efficiency

The transition from vacuum tube-based systems to solid-state technology has revolutionised RF generation. GaN FETs offer increased efficiency, reduced heat, and smaller, more reliable designs. Solid-state systems also extend lifespans and lower operational costs, and with recent advances now enabling them to handle power levels previously managed only by tube-based systems. Operating active devices as switches leads to higher efficiency but lower linearity, which is an acceptable trade-off in many RF applications where precise linear amplification is not required.

Class E generators can achieve efficiencies of between 85% and 95% and offer simple designs, making them well-suited for RF heating and plasma generation. Class F generators can theoretically exceed 90% efficiency and are suitable for high-power output at RF frequencies where linearity is less critical. Class D half-bridge generators are frequently used at frequencies like 13.56 MHz in industrial RF heating and plasma generation but become less efficient at higher frequencies due to increased switching losses.

Conclusion

The development of high-efficiency self-oscillating Class E RF generators is transforming applications within the sub-100 MHz region. By harnessing the advantages of GaN technology and innovative design approaches, these generators can deliver exceptional performance. Their ability to generate high-voltage RF energy efficiently and reliably will help to open up significant new possibilities, as well as boosting existing technologies across multiple sectors.

Before implementing these systems, readers are advised to consult detailed engineering texts and technical resources to address any specific design challenges and safety considerations.

About the Author

Tolga Aydemir is principal electronics consultant at 42 Technology, a product design and innovation consultancy based near Cambridge, UK. He has spent over 25 years in product development companies and research centres, and has significant experience in designing analogue electronics, power systems and embedded systems. Tolga is particularly focused on power electronics and analogue sensor interface development, and holds several patents in electricity metering and light control sectors.

www.42T.com

How Electronics Components support Hydrogen Solutions

Which active components fit well into applications for green hydrogen systems – in electrolyzers and fuel cells? Thyristors, IGBTs or MOSFETs? Wide Bandgap Semiconductors or Silicon? And which factors are important to know as well? This story will provide a short glimpse and give some first insights.

By Steve Albuquerque, Asia Region Business Development Manager for Energy Innovation, Future Electronics

The basic process of hydrolysis is the same, whether it is implemented in a small-scale local production facility, such as a roadside hydrogen refueling station consuming less than 500 kW, or a bulk hydrogen manufacturing plant potentially consuming 20 MW or more. A single electrolysis cell, which separates water into hydrogen and oxygen, operates at a forward voltage of around 1.8 V - 1.9 V, depending on the temperature and the chemical additives used to enhance the electrolyte. Current densities in the electrolyte range up to 0.5 A/cm². A direct current of 1,000 A can drive a cell with an area of 2,000 cm², generating roughly 1 kg of gaseous hydrogen per day [1].

Given that this basic chemical process has been well understood for many years, where is the scope to achieve future cost reductions and efficiency improvements? Currently, the cost of hydrogen produced via electrolysis ranges from $4 to $7 per kilogram, depending on the electricity price and electrolyzer efficiency. The US Department of Energy (DoE) has set a goal for this cost to fall to $2 per kilogram by 2025, and $1 per kilogram by 2030.

Achieving these cost reduction targets will require substantial improvements in electrolyzer efficiency as well as improved economies of scale resulting from the large-scale deployment of electrolysis plants.

Some of the efficiency gains for electrolysis plants will have to come from more efficient power conversion systems. And this is

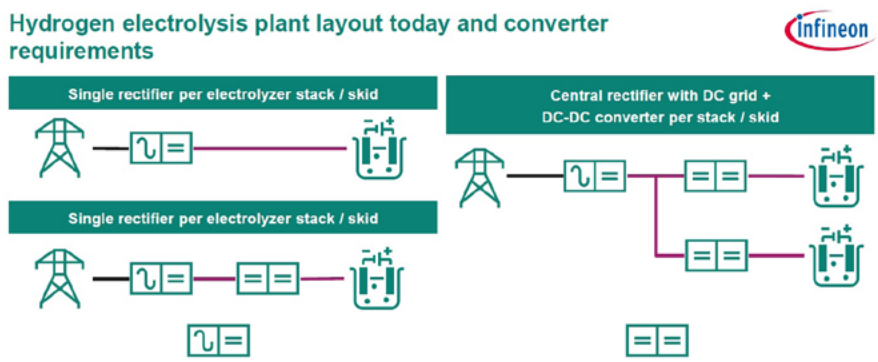

Figure 1: Typical hydrolyser plant configurations in AC/DC-coupled settings. (Image credit: Infineon)

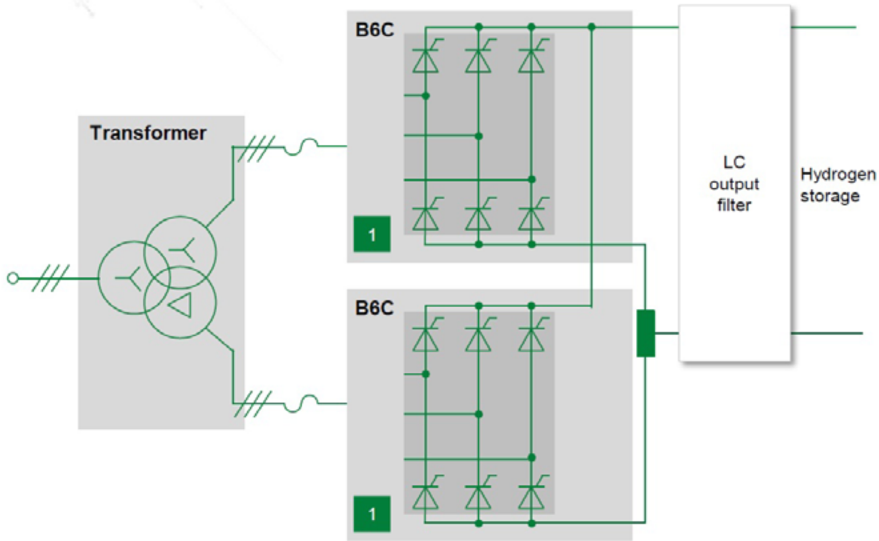

Figure 2: A thyristor-controlled B12C rectifier driven by a dedicated transformer. (Image credit: Littelfuse)

Electrolysis is a chemical operation, but it requires large amounts of electric power, either drawn from the grid or directly from wind turbines in so called 'AC/DC-coupled' power systems, or directly from solar farms and battery storage in DC/DC-coupled systems. The high-voltage power conversion equipment required to deliver the correct input to large electrolysis plants consuming megawatts of power has traditionally been the domain of a few global giant manufacturers such as ABB, Siemens and Schneider Electric. The growth in demand for electrolysis plants is opening up opportunities not only for these incumbents but also for smaller companies which have expertise in high-voltage power equipment manufacturing.

In the high-voltage equipment market, established and new suppliers will be judged by their customers – the hydrolysis plant operators – on four crucial criteria:

- Power quality
- Efficiency
- Reliability
- Cost

This creates an opening for electronics component manufacturers to advance their position by providing products which help equipment manufacturers to improve their products on any one or more of these criteria. This is leading to a new wave of innovation at component level.

sharpening the industry's focus on the improved component offerings from the main suppliers to high-voltage equipment manufacturers, such as Infineon and Littelfuse.

AC/DC-coupled Systems: Battle between Thyristors and IGBT Switches

For instance, in ac-dc coupled power systems, electrolysis plants adopt a range of configurations of the power conversion system (see Figure 1), typically based on either a diode/thyristor rectifier topology, or an IGBT based active front end (AFE) topology. AFE rectifiers can be operated at unity power factor, and produce total harmonic distortion (THD) of less than 5%.

For decades, the dominant topology in AC/DC-coupled electrolysis has been the thyristor-based 12- or 24-pulse system (see Figure 2). The main benefits of these architectures are robustness, high efficiency levels, and high current density. Thyristor rectifiers are particularly useful in high-power applications consuming more than 1 MW. Even high system power configurations operating at more than 50 MW can be efficiently implemented with an array of high-power thyristors and diode discs. Thyristor-based designs have been in operation in the field for decades, and the press-pack devices used in them offer superior power and thermal attributes.

In some industrial electrolyzers the current flowing through the rectifier can be in a range between 1.5 kA and 2.0 kA. For such high-power systems, both Littelfuse and Infineon offer integrated power solutions called power stacks, power blocks and power discs. Littelfuse offers the N1718NC200 phase-controlled thyristor capsule for up to 2.0 kA applications.

For high-voltage electrolyzers, Infineon supplies a component choice for any choice of topology. This includes AFE rectifiers, which can use its TRENCHSTOP 7 IGBT technology and/or CoolSiC silicon carbide (SiC) MOSFETs at lower power levels up to 100 kW, and IGBT-based PrimePACK products at up to 5 MW.

Thyristor versus IGBT: the pros and cons

Efficiency: IGBT systems offer higher energy efficiency than thyristor rectifiers. In green hydrogen electrolysis, in which it is important to maximize efficiency, IGBTs can minimize energy loss during power conversion.

Current and voltage handling: Thyristor rectifiers are more suitable for large-scale hydrogen electrolysis plants as they can handle higher currents and voltages. Although IGBTs are efficient, thyristors excel at managing high power levels, making them ideal for extensive hydrogen production systems.

Control and precision: IGBTs provide more power control and precision than thyristors. IGBT systems also provide greater flexibility in the control of voltage and current, ensuring the smooth and efficient operation of hydrogen electrolysis equipment.

As many countries work towards the achievement of ambitious net zero emissions targets for 2050, the development of green hydrogen power systems and hydrogen fuel supplies is also gathering momentum. This reflects the lack of constraint on the use of hydrogen, the most abundant element available for human use.

The majority of hydrogen produced today is made by splitting carbon from methane, but that produces carbon emissions. Zero-emission 'green hydrogen' comes from electrolysis, using clean electricity (from wind, solar or hydro sources) to split water into hydrogen and oxygen. Unlike batteries, which are unable to store large quantities of electricity for an extended period, hydrogen can be stored in large amounts for a long time. This makes it an ideal green storage solution for excess renewable energy.

Hydrogen has flexible uses: it can catalyze with oxygen to produce heat, or be fed into a fuel cell to make electricity. In a fuel cell, hydrogen has the potential to provide clean power for domestic use, as well as manufacturing, transportation, and more. Hydrogen fuel can also complement wind and solar energy generation, providing a green energy storage solution to balance the intermittency of the renewable sources.

Industry watchers are now forecasting strong growth in the hydrogen industry. The Hydrogen Insights 2024 report, published by the Hydrogen Council, shows that the global hydrogen project pipeline grew by a factor of seven between 2020 and May 2024, from 228 projects to 1,572 projects [2]. Investment committed to projects at the final investment decision stage also grew from around \$10bn across 102 projects in 2020 to \$75bn across 434 projects in 2024.

China has stated the aim of having 50,000 hydrogen-powered vehicles on the road by 2025, while the European Union aims to produce 10 million tons of green hydrogen – powered by renewable energy sources – by 2030.

Installation and maintenance: IGBT systems are typically smaller and easier to install than thyristor rectifiers. However, thyristors offer excellent durability and require less maintenance, making them a cost-effective option for large-scale industrial hydrogen production plants.

Both IGBT- and thyristor rectifier-based topologies play a role in optimizing the efficiency and performance of green hydrogen electrolysis systems. Understanding the advantages of each technology can help the manufacturer to choose the correct option for hydrogen production requirements.

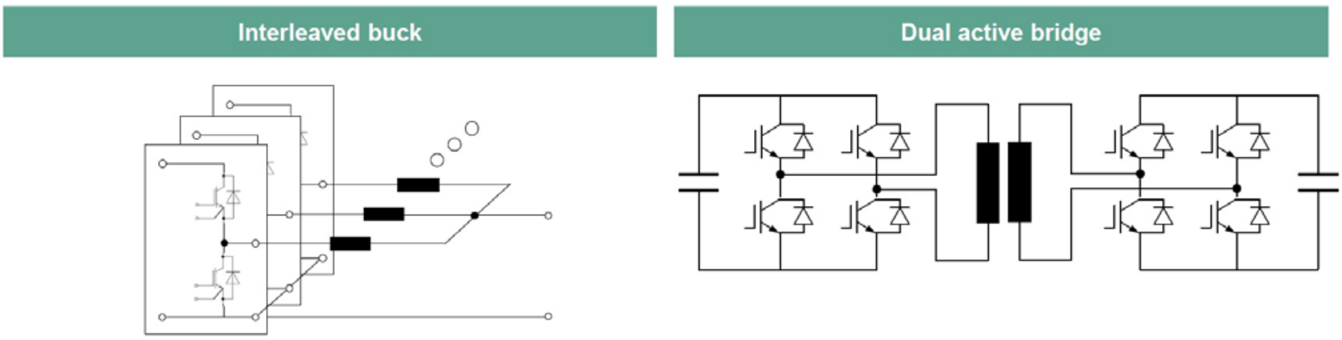

Figure 3: Topologies for conversion in hydrolysers' DC/DC-coupled conversion systems. (Image credit: Infineon)

DC/DC-coupled Systems: Wide Bandgap Innovation

In DC/DC-coupled systems powered by solar energy and/or batteries, typical topologies used for power conversion in hydrolysers are Interleaved buck and Dual active bridge (see Figure 3). Here too, component innovation is helping power equipment manufacturers to meet the market need for higher efficiency and reliability at lower system cost. For instance, Infineon is enabling manufacturers to take advantage of the superior electrical and thermal attributes of SiC MOSFETs with a new CoolSiC FET series which offers a breakdown voltage rating of up to 2,000 V.

Supplied in an HCC package with 14 mm/5.5 mm creepage/clearance distances, the IMYH200RxxxM1H MOSFETs are available with on-resistance as low as 12 mΩ. Use of these devices in electrolysis gives benefits including:

- Low conduction and switching losses
- Low reverse-recovery loss
- Excellent thermal performance
- Robust body diode for hard commutation

While these discrete devices are suitable for electrolyzers operating at 10 kW - 100 kW, integrated modules are available for use in higher-power applications of 1 MW and more. Infineon has extended the capability of its PrimePACK 3+ modules with its latest IGBT7 family, which has devices with a high 2,300 V breakdown voltage rating.

The IGBT7 devices are rated for over-temperature operation, and provide very high current density in their 247 mm x 89 mm x 38 mm form factor. For instance, the FF2400R12IP7 PrimePACK module supports currents up to 2.4 kA and voltages up to 1,200V in an interleaved buck converter.

In the dual active bridge topology, Infineon solutions include the FF2000XTR33T2M1 SiC MOSFET module in an XHP package, supporting 3.3 kV operation and featuring on-resistance of just 2 mΩ, while the FF1800R23IE7 IGBT7 module provides 2.3 kV/1.8 kA ratings.

Innovation in Power Components contributes to Growth in the Hydrogen Market

The aggressive hydrogen cost-reduction targets set by the US DoE reflect the role of hydrogen production as a key enabling technology for the adoption of hydrogen and fuel cell technologies in applications including stationary power, portable power, and transportation.

The achievement of the 1:1:1 target – $1 for 1kg of hydrogen in one decade – will depend on advances in technology throughout the hydrolyser process, as well as expanding deployments to produce economies of scale.

Continual improvements in power component efficiency and the widening range of product and package options will give the manufacturers of power equipment for electrolysis plants greater scope to create value and enable the growth in this new fuel type to accelerate.

References:

[1] Hydrolysis process description from a Littelfuse white paper, 'Fast-Charging Commercial Vehicles - A Megawatt Application Similar to Electrolysis', by Martin Schulz.

[2] Hydrogen Insights, at https://hydrogencouncil.com/wp-content/uploads/2024/09/Hydrogen-Insights-2024.pdf

www.futureelectronics.com

Advert

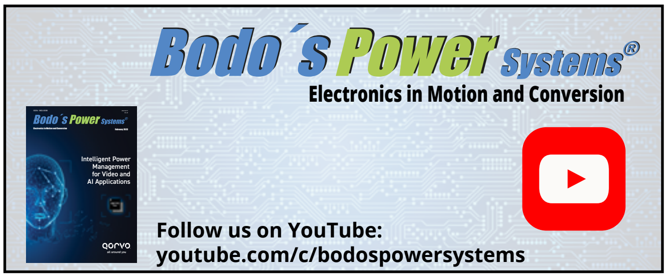

Driving a High-Side MOSFET Input Switch Using Active Low Output for System Power Cycling

Applications such as wireless transceivers where systems are placed in remote areas and usually powered with a battery require continuous operation since they are rarely visited and intervened. A system reset is required after persistent inactivity or a system hang-up to restore operation. This can be achieved by cutting off the supply voltage, disconnecting it from the system, and connecting it again to initiate a restart. This article discusses methods and techniques for using the active low output of a supervisory circuit to drive a high-side input switch to execute a system power cycle.

By Niño Angelo Pesigan, Product Applications Engineer, Ron Rogelio Peralta, Product Applications Engineer, and Noel Tenorio, Product Applications Engineer, all Analog Devices

One way to improve the reliability and robustness of electronic systems is to implement protection mechanisms that can detect faults and respond promptly. These mechanisms function as safeguards, mitigating potential damage and ensuring the proper function of a system. Power cycling is a method to ensure proper operation and protect systems and is generally conducted on unresponsive and inactive systems to allow them to work continuously. Power cycling uses a power switch that opens the path between the power supply input and the downstream electronic system, and then closes the path to initiate a system restart. Once the microcontroller unit (MCU) of the system becomes unresponsive, the system will enter reset mode and begin power cycling if inactivity persists.

The most common way of implementing a high-side power path or input switch is by using a MOSFET. Either an N-channel or P-channel MOSFET can be used as an input switch, each with a different driving requirement. Driving an N-channel MOSFET as a high-side switch is a little complicated - thus, a P-channel MOSFET is commonly preferred.

Supervisory circuits can easily sense system inactivity by monitoring the voltage supply and/or using a watchdog timer to detect the absence of pulses. The watchdog timer function enhances the capabilities of supervisory circuits as comprehensive protection solutions. Once inactivity is detected, the watchdog timer asserts a reset output, which is typically an active low signal. This signal can be used to put the microcontroller into reset mode or trigger a nonmaskable interrupt to take corrective action. While an active low output is primarily used to reset the microcontroller, in some cases, such as when the system is unresponsive for too long, it is desirable to power cycle. This can be achieved using various techniques to drive a high-side P-channel MOSFET input switch from a supervisory circuit active low output for optimal system reliability.

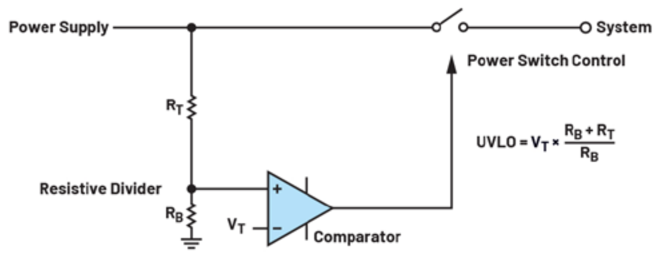

Figure 1: An example of a high-side input switch implementation to protect the system from malfunction during a brownout condition.

Using a MOSFET as a High-Side Input Switch

Figure 1 shows an application circuit using a high-side input switch to protect the downstream electronic system from errors during brownout conditions. A MOSFET is a considerable choice to be used as a system high-side switch. The appropriate voltage and current rating can easily be selected for the application.

A high-side input switch can be an N-channel or a P-channel MOSFET. The N-channel MOSFET switch opens and disconnects the supply voltage when its gate voltage is low. To completely close an N-channel MOSFET and connect the supply to the downstream electronic system, the gate voltage must be higher than the supply by at least the MOSFET threshold voltage. This requires additional circuitry such as a charge pump when using an N-channel MOSFET as a high-side input switch. Some protection circuits integrate a comparator and a charge pump to drive a high-side N-channel MOSFET while keeping the solution simple. Using a P-channel MOSFET as a high-side input switch does not require a charge pump, but the polarity is reversed. This is a common approach for many applications due to its simplicity.

Supervisory Circuit Output to Drive the Input Switch

When utilizing a P-channel MOSFET in a circuit, it is important to first establish the appropriate biasing conditions for the gate, source, and drain terminals. The gate-source voltage (V_{GS}) plays a key role in controlling the conduction of the MOSFET. In the case of a P-channel MOSFET, the gate voltage must be lower than the source voltage by at least the threshold voltage. This negative bias ensures that the P-channel MOSFET is biased into its active region, allowing the current to flow from the source to drain. Additionally, the gate-source threshold voltage ($V_{GS(th)}$) determines the minimum voltage between the gate and source terminals required to create a conducting channel. For a P-channel MOSFET, $V_{GS(th)}$ is typically specified as a negative value, indicating that the gate voltage needs to be sufficiently negative with respect to the source to allow conduction. Another important consideration is the drain-source voltage (V_{DS}), which is the voltage applied across the drain and source terminals. It is essential to operate the MOSFET within the specified V_{DS} limits to prevent damage to the device.

Voltage monitors or supervisory circuits can provide two options for their logic level output: an active low and an active high output signal. On one hand, active low means the output asserts low when the input condition is true and satisfied, and deasserts high when the input condition is false. On the other hand, active high asserts high when the input condition is true and deasserts low when the input condition is false and not satisfied. Since the most common

use of supervisory circuits is for microcontroller reset, active low output is used to pull the reset pin of the microcontroller low during faults. Driving a P-channel MOSFET using an active high output is straightforward, especially for open-drain topology.

The active high output of the supervisory circuit is connected to the gate of the P-channel MOSFET. When the monitored voltage is below the specified threshold, the OUT pin pulls the gate low, turning on the P-channel MOSFET. This connects the load to the supply voltage. When the monitored voltage exceeds the threshold, the OUT pin goes high, turning off the P-channel MOSFET and disconnecting the load from the supply voltage.

In Figure 2, the MAX16052, a high voltage adjustable sequencing and supervisory circuit is used as an overvoltage protection circuit. The OUT pin of the device is directly connected to the gate of the P-channel MOSFET. The source of the P-channel MOSFET is connected to the input voltage, and the drain is connected to the load. An external pull-up resistor is connected between V_{CC} and the gate of the P-channel MOSFET to keep the gate high when the OUT pin is low.

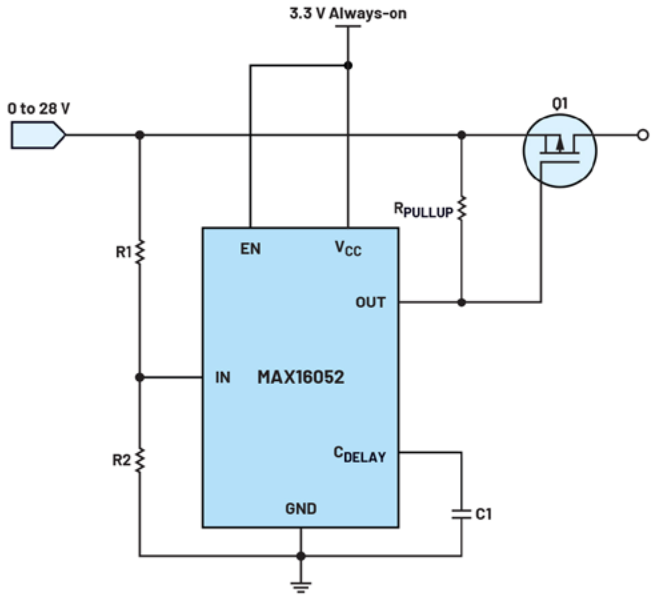

Figure 2: A P-channel MOSFET used as a high-side input switch for overvoltage protection.

When the monitored voltage is below the MAX16052's specified fixed threshold, the OUT pin pulls the gate pin low, causing the P-channel MOSFET switch to be in a short-circuited state or on state. When the monitored voltage exceeds the threshold, the OUT pin goes high, turning off the P-channel MOSFET and disconnecting the load from the supply voltage.

In some applications, the desired supervisory specification may only be available with an active low output. This means that the output signal is low when the monitored condition is met. In these cases, it is necessary to use techniques to control the input switch with an active low output. For example, in a system where the microcontroller needs to be reset after 32 s of inactivity and the system needs to be power cycled after 128 s of inactivity persistence, a watchdog timer can be used to detect the inactivity through its watchdog input (WDI) pin. The watchdog output (WDO) goes low when there is no pulse or transition detected for a certain period of time (watchdog timeout, t_{WD}). The MAX16155 nanopower supervisor with watchdog timer has variants with the desired watchdog timeout of 32 s and 128 s, respectively. Two watchdog timers are required to achieve the desired functionality - one to reset the microcontroller and one to initiate the power cycling routine shown in Figure 3. The primary challenge is determining how to use the low output of the watchdog timer variants to open the input switch during inactivity or system unresponsive state for power cycling.

NPN Bipolar Junction Transistor as a Driving Circuit

One approach to drive the P-channel high-side switch is to use an NPN bipolar junction transistor (BJT) as shown in Figure 4. This circuit forms an inverter that converts the active low signal coming from the watchdog output into a high logic signal required by the P-channel MOSFET switch.

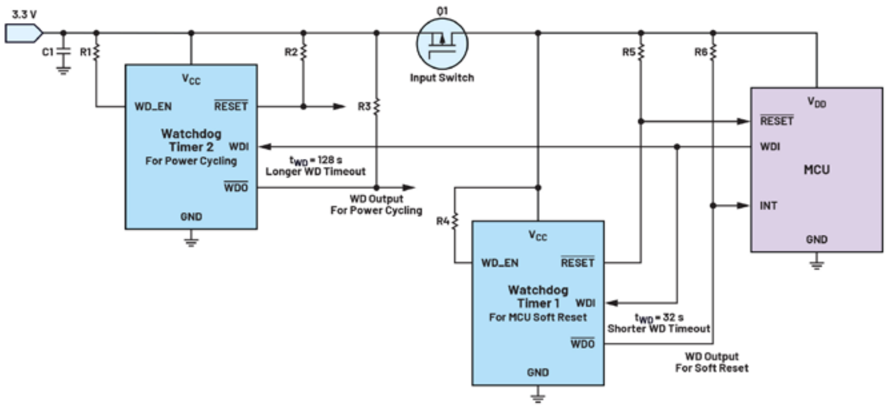

Figure 3: Two MAX16155 watchdog timers with different watchdog timeout are utilized - one to do a soft reset and another one to do power cycling

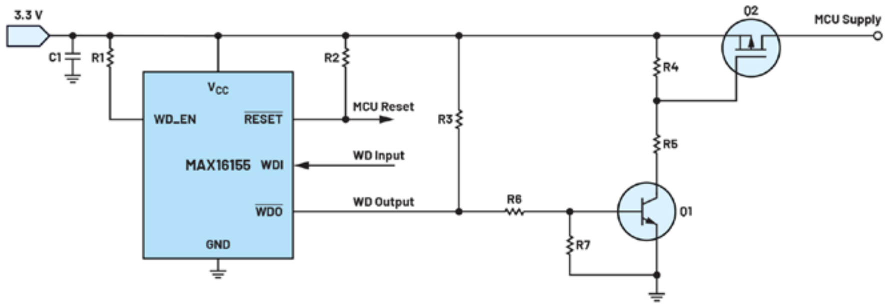

Figure 4: Using an NPN bipolar junction transistor (Q1) in driving a P-channel MOSFET (Q2) from an active low output.

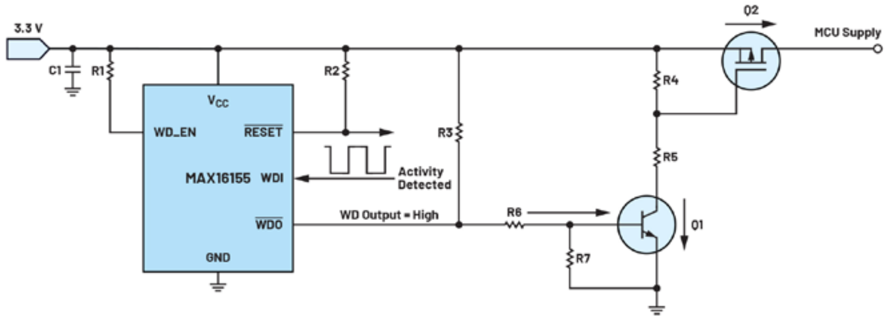

Figure 5: Current flow at normal operation - the system is active.

When the system is active, the watchdog output of the MAX16155 WDO pin is in its idle state, which is normally high. It is then connected with a current limiting resistor network to the base pin of the driving transistor. The normally high output of the WDO pin supplies the necessary base-emitter voltage as the control input for the NPN bipolar junction transistor. It establishes enough voltage across the base-emitter junction, causing the transistor to enter its conducting state.

A resistor divider is connected to the gate pin and source pin of the high-side MOSFET switch to control its gate-source voltage (V_{GS}). This gate-source voltage determines whether the MOSFET remains in its on or off state. When the NPN bipolar junction transistor is activated by the WDO pin, current flows through the transistor. This pulls the resistor divider low to GND, which changes the voltage at the junction point in the resistor divider. This voltage is then applied to the gate pin of the high-side MOSFET. This produces a potential difference where the gate pin is at a lower potential than the source pin, which effectively turns on the MOSFET. With the MOSFET in its on state, the power supply is provided to the system microprocessor or the load. Figure 5 shows the current flow when the system is active and the power supply is provided through the switch, Q2.

However, when the microprocessor becomes unresponsive or fails to provide input pulses within the predefined timeout period of the MAX16155 watchdog timer, a watchdog timeout event occurs and WDO asserts low. This consequently pulls the base of the NPN BJT Q1 to the ground, turning it off. When Q1 opens, the voltage on the gate and the source of the P-channel MOSFET Q2 will be approximately equal, which is enough to turn it off.

As shown in Figure 5, the collector pin of the NPN bipolar junction transistor is connected to the resistor divider across the high-side MOSFET. Due to the off state of the NPN bipolar junction transistor, the voltage on the junction point of the resistor divider and the gate will be approximately equal to the voltage in the source pin. This will result in a zero potential difference between the gate and the source of the MOSFET, which fails to meet the V_{GS} threshold value required to keep the MOSFET Q2 in its conducting state. Consequently, with the MOSFET now turned off, the 3.3 V supply to the microprocessor is disconnected, effectively cutting off power to the microprocessor or the load. The equivalent circuit and current flow during system inactivity and power cycling are shown in Figure 6.

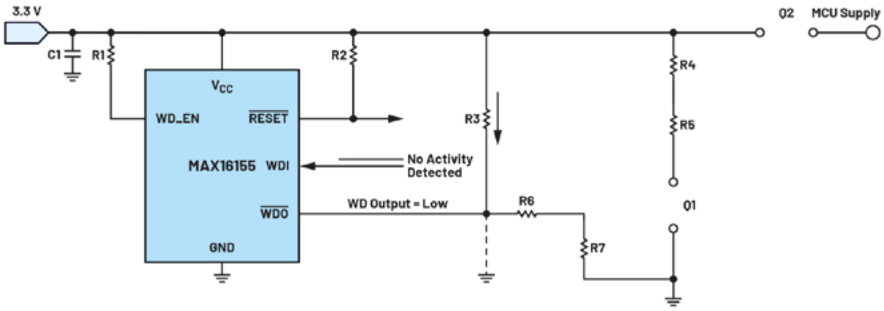

Figure 6: Current flow during system inactivity—power cycle occurs.

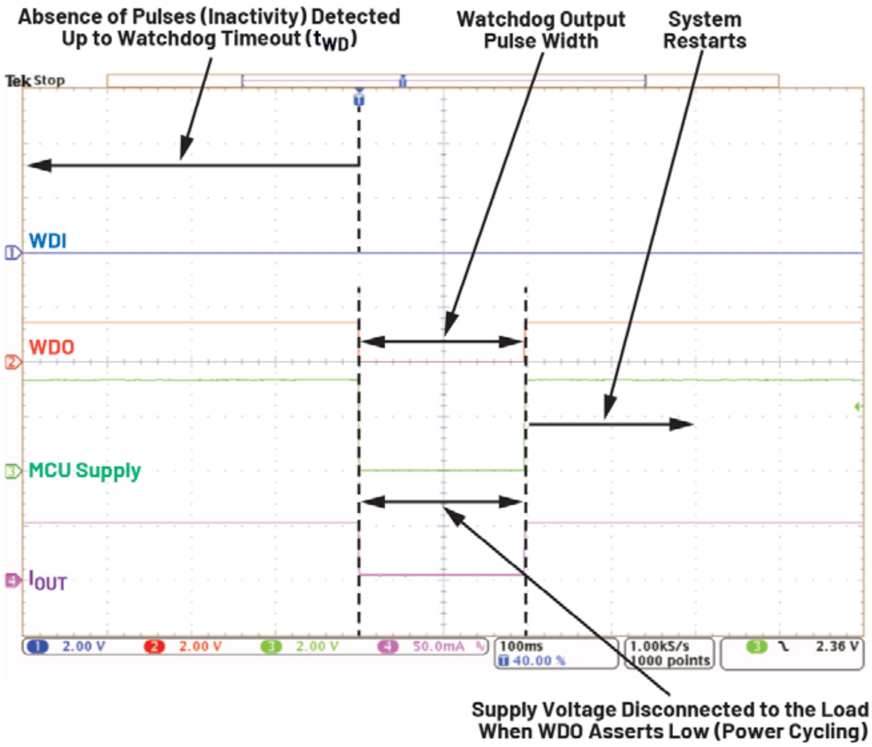

Figure 7: Signals using an NPN bipolar junction transistor in the driving circuit (CH1—WDI signal; CH2 - WDO signal; CH3 - MCU supply; CH4 - I_{OUT}).

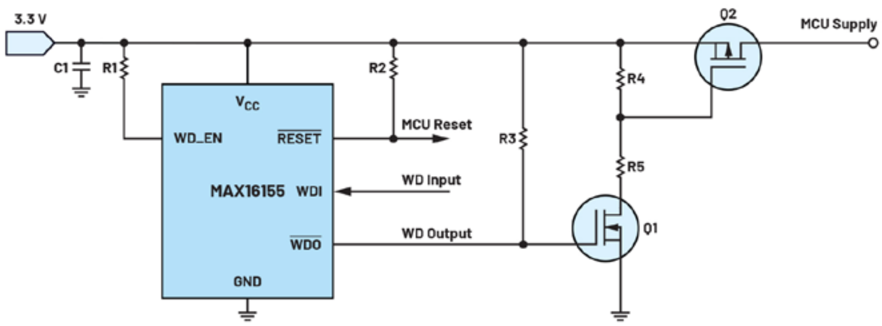

Figure 8: Using an N-channel MOSFET (Q1) in driving a P-channel MOSFET (Q2) from an active low output.

After the WDO output pulse width is completed and returns to a high voltage level, the system reverts to its normal operation. During this phase, the microprocessor resumes sending regular input pulses to the WDI pin, preventing further watchdog timeout events. The NPN bipolar junction transistor returns to its active state, allowing the high-side MOSFET to remain ON, ensuring an uninterrupted power supply to the microprocessor or load. Figure 7 shows the waveforms during the power cycling event using the NPN bipolar transistor. As shown in CH1, there are no transitions detected in the WDI signal which implies system inactivity. After the timeout period, the WDO signal in CH2 asserts low, and during this time, the high-side input switch Q1 opens. Thus, there is no voltage measured in CH3 and the MCU supply voltage and system restart is initiated. CH4 is the output current that is drawn by the load that turned to zero amperes showing that the load was disconnected to the supply voltage.

One of the major advantages of using an NPN bipolar junction transistor as the driver of the high-side switch is the lower cost of bipolar junction transistors. However, biasing the NPN bipolar junction transistor requires proper tuning with the help of additional external components such as resistors.

Using an N-Channel MOSFET as a Driving Circuit

An alternative driving circuit using an N-channel MOSFET can be implemented for controlling the high-side P-channel MOSFET. This approach has several advantages over using a bipolar transistor.

The N-channel MOSFET's low on-resistance ensures minimal voltage drop across the device, leading to reduced power dissipation and increased energy efficiency. The MOSFET's fast switching capabilities enable quicker response times, enhancing the supervisory system's real-time performance. Another advantage that the MOSFET can offer is that it exhibits reduced switching losses and higher operating frequencies. This allows smooth and efficient operation, resulting in preserving energy such as in battery-powered applications.

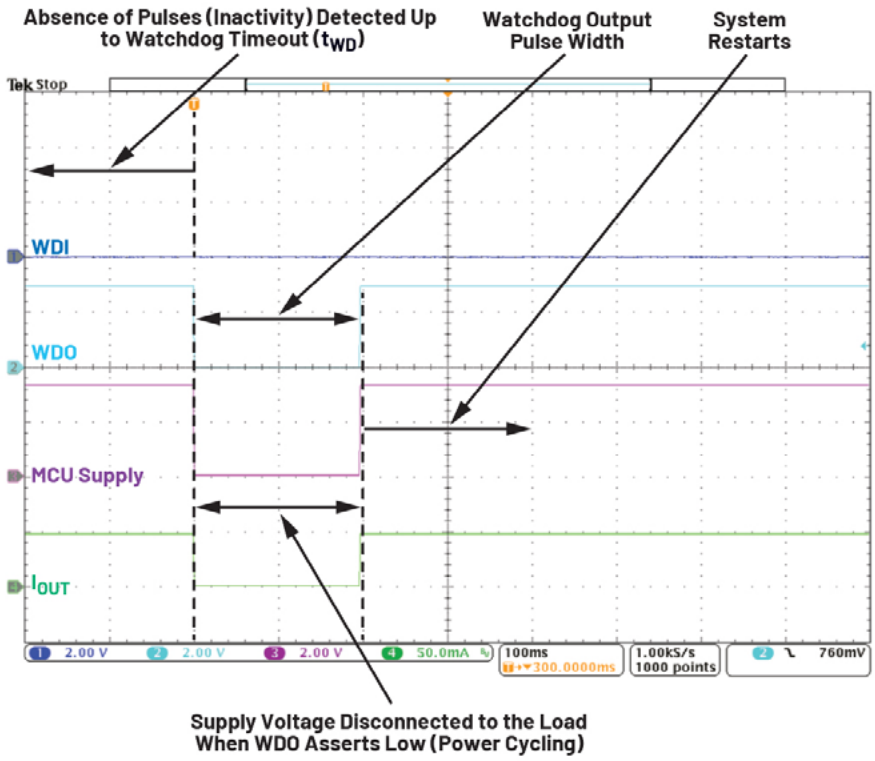

Figure 9: Signals using an N-channel MOSFET in the driving circuit (CH1 - WDI signal; CH2 - WDO signal; CH3 - MCU supply; CH4 - I_{OUT}).

Moreover, the gate-drive requirements are less demanding than those of a bipolar junction transistor, simplifying the driving circuitry and reducing the number of components needed. The watchdog output can directly drive the gate of the N-channel MOSFET shown in Figure 8. The pull-up voltage of the WDO should meet the gate threshold voltage $V_{GS(th)}$ of the N-channel MOSFET to work properly. A logic high output voltage of the WDO when the system is active will turn on Q1, which will consequently turn on Q2, delivering power to the system. Like in the case of the bipolar transistor, a logic low output level from the WDO pin during system inactivity will turn off Q1 and open Q2, cutting off the supply voltage to the system. The behavior of the signals during power cycling using the N-channel MOSFET as a driving circuit is shown in the captured waveform in Figure 9.

The discussed approach in driving high-side switches is beneficial not only on wireless transceivers, but also on other applications that require a power cycling routine in system protection during faults, such as overvoltage and overcurrent in functional and intrinsic safety systems. The sensing stage depends on what condition is required for the power cycle to take place. It can be a voltage supervisor in detecting voltage faults, or current sensor in preventing overcurrent, and other techniques. This article discusses how sensory and supervisory devices with active low output can be used in protecting downstream systems with power cycling.

Conclusion

There are several techniques for using the active-low signal from a supervisory circuit to drive a high-side switch for power cycling. Using an NPN bipolar transistor with additional components is a lower cost option that meets the requirements for driving the P-channel MOSFET input switch. On the other hand, using an N-channel MOSFET requires fewer components and is easier to implement, but it is more expensive overall. N-channel MOSFETs also have advantages when used as switches at high frequencies. Both approaches are well-proven and provide design advantages for system power cycling.

www.analog.com

Automotive grade residual Current Monitoring Sensor

LEM has designed an automotive grade residual current monitoring (RCM) type B sensor for bi-directional OBCs with ASIL B capabilities according to ISO26262 for transformer-less on-board chargers (OBCs). This sensor, called CDT, complies with all the relevant safety standards. The RCM type B sensor enables designers to react to the new ISO5474 Part 2 standard for AC power transfer. The standard focuses on electrically propelled road vehicles and outlines the functional and safety requirements for power transfer between the vehicle and an external electric circuit using AC. Part of a series that operates in conjunction with ISO5474 Part 1, the new standard covers conductive charging requirements for modes 2 and 3 according to IEC 61851-1, reverse power transfer through on-board standard socket-outlets or EV plugs, and voltages up to 1000V AC. The CDT detects differences in current between two points, identifying such faults as short circuits and enabling rapid isolation of faulty sections to prevent damage. LEM's CDT sensor is suited for RCM type B for bi-directional OBCs, where residual currents are detected and monitored, including AC and DC leakage currents. Using LEM's patented fluxgate technology the CDT sensor offers a level of accuracy of ± 0.5 mA @ 5 mA. The device also provides functions on the secured Serial Peripheral Interface (SPI) bus including dynamic fault selection, monitoring of T°C, leakage value and supply monitoring, but it also provides diagnostic functions, and it is able to work equally effectively with single-phase and 3-phase AC.

www.lem.com

800 V GaN Inverter with 30 kW/l Power Density

Cambridge GaN Devices (CGD) and IFP Energies nouvelles (IFPEN), a French public research and training organization in the fields of energy, transport and the environment, have developed a demo which confirms the suitability of CGD's ICeGaN®650 V GaN ICs in a multi-level, 800 VDC inverter. The demo delivers a power density of 30 kW/l, which is greater than can be achieved by more expensive, state-of-the-art SiC-based devices. The inverter realization also demonstrates the ease of paralleling that ICeGaN technology enables; each inverter node has three 25 mΩ / 650 V ICeGaN ICs – 36 devices in total – in parallel. This multi-level GaN Inverters can power electric motors to over 100 kW peak, 75 kW continuous power. The CGD/IFPEN demo features: a high voltage input of up to 800 V_{DC}, 3-phase output, a peak current of 125 A_{RMS} for 10 s or 180 A_{Peak} and a continuous current of 85 ARMS continuous (120 A_{Peak}). The improvement in the efficiency of the traction inverter leads to an increase in battery range and a reduction in charging cycles. As GaN transistors can operate at much higher frequencies than silicon transistors, the iron losses in the motor, particularly in the case of machines with low inductances are reduced. The 3-level topology reduces EMI and enhances the reliability of the system. In terms of thermal management insulated metallized substrate boards featuring an aluminium core facilitate thermal dissipation for adequate operating temperatures, and this extends the lifespan of the system and associated GaN devices. The modular design facilitates scalability and adaptability for varying system requirements.

www.camgandevices.com

600 W Open Frame Power Supply for Medical and Industrial Applications

Murata Manufacturing has introduced the PQC600 open-frame AC to DC power supply, which caters to the needs of the latest medical and industrial applications, such as hospital beds, dentist chairs, medical equipment, and industrial process machinery. It offers 600 W of power within a package that is less than 1U in height and is certified to the IEC 60601-1 Edition 3 medical safety standard, which includes 2 Means of Patient Protection (MOPP) from primary to secondary, 1 MOPP from the chassis to ground and 1 MOPP from output to chassis. Additionally, the PQC600 complies with the IEC 60601-1-2 4th Edition for EMC standards, ensuring robust electromagnetic compatibility, and is suitable for use with medical devices that have Type B or Type BF applied parts. With a 600W forced-air cooling design, it achieves an efficiency of 95 % at full load. The power supply features an interleaved Power Factor Correction (PFC) and back-end synchronous rectification. Furthermore, the power supply includes a droop current sharing feature, enabling multiple units to be configured in parallel for greater power scalability.

www.murata.com

SiC Schottky Barrier Diodes for High-Voltage xEV Systems

ROHM Semiconductor announced surface mount SiC Schottky barrier diodes (SBDs) that improve insulation resistance by increasing

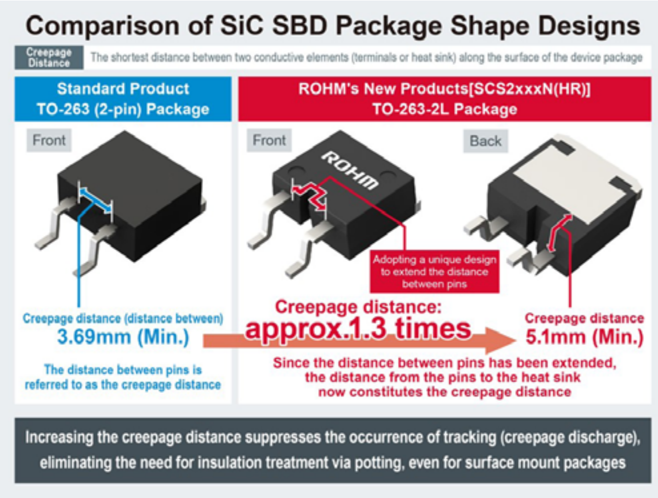

the creepage distance between terminals. The initial lineup includes eight models (SCS2xxxNHR; AEC-Q101 qualified) for automotive applications such as onboard chargers (OBCs), which will soon be supplemented by eight additional models (SCS2xxxN) for industrial equipment such as FA devices and PV inverters. Adopting a specific package shape, it achieves a minimum creepage distance of 5.1 mm. These products utilize an original design that removes the center pin previously located at the bottom of the package, extending the creepage distance to a minimum of 5.1 mm, approximately 1.3 times greater than standard products. This minimizes the possibility of tracking (creepage discharge) between terminals, eliminating the need for insulation treatment through resin potting when surface mounting the device on circuit boards in high-voltage applications. Additionally, the devices can be mounted on the same land pattern as standard and conventional TO-263 package products, allowing the replacement on existing circuit boards. Two voltage ratings are offered – 650 V and 1200 V – supporting 400 V systems commonly used in xEVs, as well as higher voltage systems expected to gain wider adoption in the future.

www.rohm.com

Facilitating SiC and GaN Power Testing

The Italian company CREA (Collaudi Elettronici Automatizzati) – a subsidiary of Advantest Europe – presented its solution for a variety of power devices, including SiC and GaN power testing on wafer, single-die, substrate, PKG, and module, typically used in industrial and automotive applications. PCI (Probe Card Interface) technology, patented by CREA, is a high-volume manufacturing test solution designed to work seamlessly with the CREA MT tester family. This combination enables high-power static, dynamic, and short circuit testing for Si, SiC, and GaN bare dies, particularly in Known Good Die (KGD) applications. PCI hardware allows monitoring the power levels maintained by each probe card needle in real-time, allowing test engineers to predict potential Device Under Test (DUT) failures during the test phase. Whenever a device failure is predicted, the PCI can react immediately (within 300 ns) by shutting off the probe card's power supply, safeguarding the equipment hardware (probe card, instruments) and the DUT. The system supports voltages up to 10 kV with a current capability up to 15 kA.

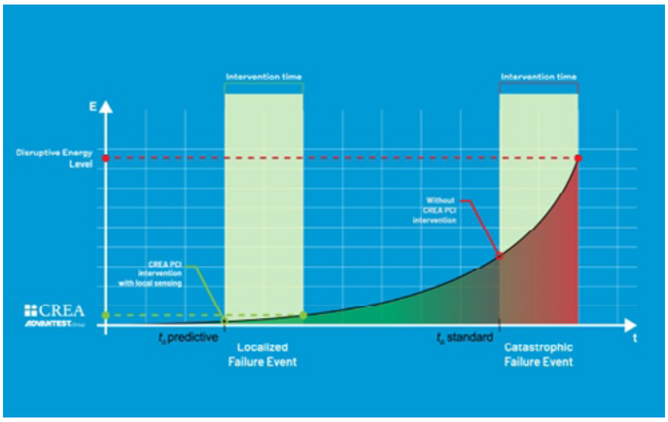

www.crea-test.com

Automotive-Grade SiC MOSFETs in TC3PAK Package

Inventchip Technology released four automotive-grade SiC MOSFETs in the TC3PAK package: IV2Q12080K1Z, IV2Q12040K1Z, IV3Q12035K1Z and IV3Q12021K1Z. They are rated at 1200 V with resistance values of 80 mΩ, 40 mΩ, 35 mΩ and 21 mΩ respectively. The TC3PAK package, designed for topside cooling, boasts a 125 mm² metal tab surface, significantly enhancing heat dissipation capabilities. Compared to the traditional TO-263/D2PAK package, the TC3PAK's heat dissipation area is over 200 % larger, effectively halving the thermal resistance between the case and the heatsink. This design not only improves thermal management but also facilitates a more efficient heat dissipation process. Unlike TO-263/D2PAK packages that depend on PCB for heat dissipation and conduction, TC3PAK allows direct heat conduction to a heatsink via its topside metal tab. Furthermore, the TC3PAK package is 23 % thinner, measuring under 3.6 mm in height, compared to the TO-263/D2PAK, which makes it more suitable for low profile designs. Its large lead frame can support a large die, such as a 5 mm x 6 mm die, or multiple dies, providing ample space for future power upgrades without the necessity for a new package format. The TC3PAK package is engineered for surface mounting with a top-side connection to an external heatsink and facilitates the automatic assembly of the PCB-power devices-heatsink stack.

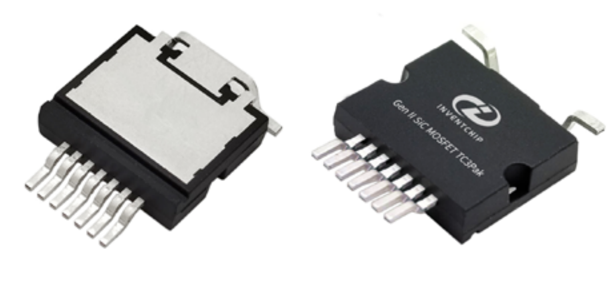

www.inventchip.com.cn

Linear FET 2 MOSFET for Hot-Swap and Battery Protection

The safe hot-swap operation in AI servers and telecom requires MOSFETs with a robust linear operating mode as well as a low $R_{DS(on)}$. Infineon Technologies addresses this challenge with its OptiMOS™ 5 Linear FET 2 – a "MOSFET designed to provide the ideal trade-off between the $R_{DS(on)}$ of a trench MOSFET and the wide safe operating area (SOA) of a classic planar MOSFET". The device prevents damage to the load by limiting the high inrush current and ensures low losses during operation. Compared to the previous generation (the OptiMOS Linear FET), the OptiMOS Linear FET 2 offers improved SOA at elevated temperatures and reduced gate leakage current, as well as a wider range of packages. This allows for more MOSFETs to be connected in parallel per controller, reducing bill-of-material (BOM) costs and offering more design flexibility due to the extended product portfolio. The 100 V OptiMOS 5 Linear FET 2 is available in a TO-leadless package (TOLL) and offers a 12 times higher SOA at 54 V at 10 ms and 3.5 times higher SOA at 100 µs compared to a standard OptiMOS 5 with similar $R_{DS(on)}$. The latter improvement is particularly important for the battery protection performed inside the battery management system (BMS) in case of a short circuit event. This enables high power density, efficiency, and reliability for battery protection which are used in a wide range of applications including power tools, e-bikes, e-scooters, forklifts, battery back-up units and battery-powered vehicles.

www.infineon.com

Hot-Swap/E-Fuse

HMI released the HL8520E, a hot-swap/E-Fuse device designed to offer protection and power control for sensitive load circuitry. The HL8520E is designed to protect systems from input transients, shorts, and voltage spikes that could damage load circuitry, while managing power delivery to enhance reliability. With an input voltage range of 2.7 V to 16 V, it supports both low- and high-voltage systems, making it suitable for diverse applications. The device can also handle up to 20 A of output current. Featuring an integrated MOSFET with an $R_{DS(on)}$ of 2.8 mΩ, the HL8520E reduces conduction losses while improving power efficiency, and thermal performance. It includes several protection features, such as over-current protection (OCP), short-circuit protection (SCP), thermal shutdown (TSD), damaged MOSFET detection, over-voltage protection (OVP), and under-voltage lockout (UVLO), safeguarding both the device and the load from electrical faults. For smoother system operation, the HL8520E allows for an external adjustable soft start, enabling controlled inrush current during startup. Additionally, the device provides configurable current limits. The response time of less than 200 ns for short-circuit protection helps detecting and mitigating fault conditions. The device comes in an LGA-26 package measuring 4 mm x 4 mm.

www.hmisemi.com

DC/DC Converters for Industrial and Railway Environments

CUI announces two high-performance isolated DC/DC converters, the PRC300 and 600 series, both designed with 4.2 kV isolation to support engineers in e-mobility, railway, and industrial industries. The PRC300 series, which is UL/EN/IEC 62368-1 certified, has several special features reinforced insulation and baseplate cooling. The PRC600 series offers 600 W of power in a compact brick package and positive and negative logic options, which is well-suited for a variety of industrial and high-voltage applications. Additional features include remote ON/OFF control and output voltage trimming. The industry standard half and full brick packages both offer a high input voltage range of 180 to 400 V_{DC} and an operating temperature ranging between -40 and +100 °C. The converters provide several protection features, including over-current, over-temperature, over-voltage, short circuit, and input under-voltage protections. In addition, they meet EN 61373 and EN 45545-2.

www.cui.com

1200 V SiC MOSFETs in Bare Die Format

Toshiba has developed the X5M007E120, a 1200 V SiC MOSFETs with an low on-resistance of 7.2 mΩ, which is particularly suited to applications within automotive traction inverters. The device has a V_{DSS} of 1200 V and is rated for a drain current (I_D) of 229 A continuously, with 458 A for pulsed operation ($I_{D\ Pulse}$). These AEC-Q100 qualified devices can operate with channel temperatures (T_{ch}) up to 175 °C. Engineering samples are expected to ship during 2025, with mass production samples scheduled to start in 2026.

www.toshiba.semicon-storage.com

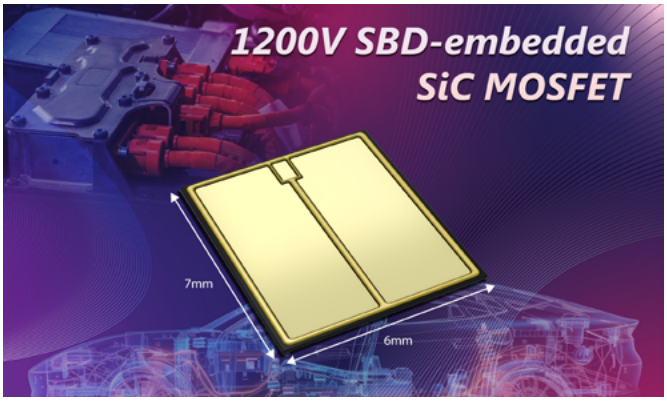

IGBTs in several different Packages for up to 1700 V

Microchip Technology now offers its IGBT 7 devices in different packages, multiple topologies, as well as current and voltage ranges. The components are available in standard D3 and D4 62 mm packages, as well as SP6C, SP1F and SP6LI packages; they are intended for power applications in solar inverters, hydrogen ecosystems, commercial and agricultural vehicles and More Electric Aircraft (MEA). Many configurations are available in the following topologies: three-level Neutral-Point Clamped (NPC), three-phase bridge, boost chopper, buck chopper, dual-common source, full-bridge, phase leg, single switch and T-type. Devices can be provided with voltages ranging from 1200 V to 1700 V while currents range from 50 A to 900 A. Claimed to operate with a "lower on-state IGBT voltage (V_{ce}), improved antiparallel diode (lower V_f) and increased current capability" these components can enable lower power losses.

www.microchip.com

High Speed & High Power DC Electronic Load

One of the features of the IT8900G/L series high power DC electronic load from ITECH is its fast current dynamic response. Compared with its predecessor, the current rise/fall speed of this device has been increased by 3-4 times, ensuring that users are able to capture even smaller fluctuations in real time when dealing with complex load changes. Especially in scenarios that require high-speed response, such as testing server power supplies, DC/DC modules, and on-board chargers (OBCs), theIT8900G/L demonstrates its processing capabilities. The IT8906G-150-600 model can provide 0...600 A under 30 kHz dynamic band load conditions. To further optimize stability in high-frequency testing, ITECH has also introduced a low-inductance test line, which significantly reduces electromagnetic interference during rapid current changes for efficient and accurate signal transmission. The device supports load testing down to 0.075 V / 60 A and 0.75 V / 600 A with an internal resistance of 0.7 mΩ, making the IT8900G/L a test tool for fuel cells, supercapacitors, and solar cells.

www.itechate.com

Advertising Index

fine power®

YOUR INNOVATION HUB

ENGINEERING HUB

Power as a core competence

for designing electronic components and systems

- Digital power control since 2008
- Wide band gap semiconductors since 2011
- Support of the entire development process

Application competence

- Automotive, industry and renewable energy
- Wireless or conductive battery charging technology
- Bidirectional converters – conductive and inductive
- Power classes up to 100kW

Services

- Circuit design and layout
- Mechanical design
- Electrical, magnetic, thermal, mechanical and EMC simulations
- Prototype construction and commissioning
- Support with qualification and series production

PERSONAL RESPONSIBILITY - FREEDOM - APPRECIATION

Join our Team:

- Application Engineer for Magnetics
- Embedded SW Development Engineer
- HW Development Engineer

Career at Finepower:

www.finepower.com